Global Premature Mortality by Dust and Pollution $PM_{2.5}$ Estimated from the MERRA-2 Aerosol Reanalysis

Alexander Yang[1,2], Qian Tan[3,4], Chamara Rajapakshe[1,5], Mian Chin[1], Hongbin Yu[1*]

[1] NASA Goddard Space Flight Center, Greenbelt, Maryland, USA

[2] Marriotts Ridge High School, Marriottsville, Maryland, USA

[3] Bay Area Environmental Research Institute, Petaluma, California, USA

[4] NASA Ames Research Center, Moffett Field, California, USA

[5] University of Maryland Baltimore County, Baltimore, Maryland, USA

*** Correspondence**
Dr. Hongbin Yu, NASA Goddard Space Flight Center
Hongbin.Yu@nasa.gov

Keywords: $PM_{2.5}$, dust, pollution, aerosol, mortality

Abstract

This study quantifies global premature deaths attributable to long-term exposure of ambient $PM_{2.5}$, or $PM_{2.5}$-attributable mortality, by dust and pollution sources. We used NASA's Modern-Era Retrospective Analysis for Research and Applications, Version 2 (MERRA-2) aerosol reanalysis product for $PM_{2.5}$ and the cause-specific relative risk (RR) from the integrated exposure-response (IER) model to estimate global $PM_{2.5}$-attributable mortality for five causes of deaths, namely ischaemic heart disease (IHD), cerebrovascular disease (CEV) or stroke, lung cancer (LC), chronic obstructive pulmonary disease (COPD), and acute lower respiratory infection (ALRI). The estimated yearly global $PM_{2.5}$-attributable mortality in 2019 amounts to 2.89 (1.38 ~ 4.48) millions, which is composed of 1.19 (0.73 ~ 1.84) million from IHD, 1.01 (0.35 ~ 1.55) million from CEV, 0.29 (0.11 ~ 0.48) million from COPD, 0.23 (0.14 ~ 0.33) million from ALRI, and 0.17 (0.04 ~ 0.28) million from LC (the numbers in parentheses represent the estimated mortality range due corresponding to RR spread at the 95% confidence interval). The mortality counts vary with geopolitical regions substantially, with the highest number of deaths occurring in Asia. China and India account for 40% and 23% of the global $PM_{2.5}$-attributable deaths, respectively. In terms of sources of $PM_{2.5}$, about 22% of the global all-cause $PM_{2.5}$-attributable deaths are caused by desert dust. The largest dust attribution is 37% for ALRI. The relative contributions of dust and pollution sources vary with the causes of deaths and geographical regions. Enforcing air pollution regulations to transfer areas from $PM_{2.5}$ nonattainment to $PM_{2.5}$ attainment can have great health benefits. Being attainable with the U.S. air quality standard (AQS) of 15 $\mu g/m^3$ globally would have avoided nearly 40% or 1.2 million premature deaths. The most recent update of $PM_{2.5}$ guideline from 10 to 5 $\mu g/m^3$ by the World Health Organization (WHO) would potentially save additional one million lives. Our study highlights the importance of distinguishing aerodynamic size from geometric size in accurately assessing the global health burden of $PM_{2.5}$ and particularly for dust. A use of geometric size in diagnosing dust $PM_{2.5}$ from the model simulation, a common approach in current health burden assessment, could

overestimate the $PM_{2.5}$ level in the dust belt by 40-170%, leading to an overestimate of global all-cause mortality by 1 million or 32%.

1 Introduction

$PM_{2.5}$, namely particulate matter (PM) with an *aerodynamic* diameter of smaller than 2.5 μm, is a major air pollutant that comes from diverse sources, such as fossil fuel combustion for industrial and residential uses, biomass burning from wildfires and crop field clearance, dust storms, biogenic and biological activities of the ecosystems, burst of ocean bubbles, and volcanic eruptions. Being over 30 times smaller than a human hair, these fine particles can easily enter our respiratory systems and cause significant health risks. The risks range from chronic cardiovascular and respiratory disease to lung cancer, and from cognitive decline to psychological distress, as suggested by a growing body of compelling evidence (Pope et al., 2002; Glinianaia et al., 2004; Pope and Dockery, 2006; Power et al., 2016; Schraufnagel, 2019; Chen and Hoek, 2020). In 2015, $PM_{2.5}$ pollution was ranked as the fifth most important risk factor contributing to global mortality (Cohen et al., 2017). Globally exposure to ambient or outdoor $PM_{2.5}$ pollution has been increasing over the past decades (Shaddick et al., 2020). Currently more than 90% of the global population is exposed to an ambient $PM_{2.5}$ level higher than the air quality guideline (AQG) of 10 μg m^{-3} for annual $PM_{2.5}$ exposure issued by the World Health Organization (WHO) in 2006 (this AQG has been updated to 5 μg m^{-3} in 2021 to better protect public health worldwide, based on extensive scientific evidence, Chen and Hoek, 2020).

Currently estimates of global health burden due to long-term exposure to ambient $PM_{2.5}$ are subject to large uncertainties. It has been estimated that the $PM_{2.5}$ level in recent years was responsible for 3-9 million premature deaths a year (Lelieveld et al., 2015; Cohen et al., 2017; Burnett et al., 2018; GBD, 2020; McDuffie et al., 2021). Major sources for this broad range of $PM_{2.5}$-attributable mortality come from both the characterization of $PM_{2.5}$ concentrations and the quantification of concentration-response functions (CRF) or relative risks (RR). Clearly, improving the estimate of $PM_{2.5}$-attributable mortality requires a great deal of collaborative effort across multiple disciplines. In this study we focus on improving the characterization of $PM_{2.5}$ by using the Modern-Era Retrospective analysis for Research and Applications, Version 2 (MERRA-2) aerosol reanalysis constrained by satellite observations of aerosol optical depth (Randles et al, 2017). We highlight the importance of using the aerodynamic diameter (D_{aer}), instead of geometric diameter (D_{geo}), to partition total dust mass into fine ($PM_{2.5}$) and coarse dust in air quality and health outcome assessment. The aerodynamic diameter D_{aer} is the diameter of a sphere with a density close to water that has the same gravitational settling velocity as the aerosol particle has (Hinds, 1999). Clearly, these two size parameters will be different if the particle has a different density and/or shape than water. In the real world, D_{geo} is always greater than D_{aer}.

Mineral dust, composed of both fine ($PM_{2.5}$) and coarse particles, has a ubiquitous presence around the globe and is the most important component of continental aerosols in terms of mass. In assessing $PM_{2.5}$ health impacts, mineral dust emitted from remote deserts must be included (Ostro et al., 2021), though many studies have largely focused on anthropogenic sources because of their proximity to dense populations. Dust affects vast regions both immediate to and far from the sources, because of its long-range transport (Yu et al., 2012, 2013, 2015a, 2015b). Although dust $PM_{2.5}$ concentration is much higher in areas adjacent to the sources than in downwind regions, the health impact of dust could be more significant in downwind populous regions (Sandstrom and Forsberg, 2008; Stafoggia et al., 2013, 2016). The most recent analysis of model simulations shows that dust alone, by shutting down all anthropogenic and fire emissions, could make ~40% of the world's population experiencing annual $PM_{2.5}$ exposure above the WHO AQG of 5 μg m^{-3} (Pai et al., 2022). Giannadaki et al. (2014)

84 estimated that dust $PM_{2.5}$ caused global mortality of 412,000, and 3.56 million years of life lost per
85 year. Recognizing the important impacts of mineral dust on human health, weather and climate, and
86 the environment and society, the World Meteorological Organization (WMO) launched its Sand and
87 Dust Storm Warning Advisory and Assessment System (SDS-WAS) in 2007 to provide science and
88 application communities with timely and quality forecasts and observations of dust storms. Several
89 regional nodes around the globe have been established. And the United Nations (UN) Global
90 Assembly has passed two resolutions to recognize the severity of the SDS problem and call on all the
91 UN entities to foster close coordination in combating this thorny problem facing us.

92 How important is dust $PM_{2.5}$ in affecting human health? Previous studies have yielded a wide range
93 of estimates of the relative contributions of dust and anthropogenic $PM_{2.5}$ to global mortality. Lim et
94 al. (2012) estimated that dust accounted for only about 2% of global total mortality in 2010. Evans et
95 al. (2013) showed that by excluding dust the estimated global mortality attributable to $PM_{2.5}$ could
96 decrease from 12.1% to 8%, suggesting that dust could account for about 33% of the $PM_{2.5}$-
97 attributable mortality. Lelieveld et al. (2015) used a global model to estimate that dust contributes to
98 11-18% of the $PM_{2.5}$-attributable mortality, with the lower fractional contribution corresponding to
99 an assumption that anthropogenic $PM_{2.5}$ was five times more toxic than dust. Clearly, all these
100 estimates depend on how accurately models can capture the dust and anthropogenic $PM_{2.5}$ partitions.

101 The characterization of dust $PM_{2.5}$ is subject to large uncertainties. Observations of size-resolved
102 dust are scarce and subjected to high uncertainties. Model simulations of the global dust cycle
103 perform poorly, due to lack of strong constraints on emissions, transport, and removals of dust
104 (Huneeus et al., 2011). Because models usually use geometric size to describe the dust particle size
105 distribution, some studies have derived dust $PM_{2.5}$ by cutting off at D_{geo} of 2.5 μm. In other studies,
106 the dust $PM_{2.5}$ is defined as particles with a diameter of smaller than 2.5 μm without clearly stating if
107 it is referred to as geometric or aerodynamic diameter. Given that the geometric size of dust particles
108 is significantly larger than the aerodynamic size, the so-derived dust $PM_{2.5}$ with the cutoff at D_{geo} of
109 2.5μm would bias high, yielding an overestimate of its health impacts. In this study we will address
110 this existing ambiguity by deriving the Modern-Era Retrospective Analysis for Research and
111 Applications, Version 2 (MERRA-2) dust and total $PM_{2.5}$ based on aerodynamic size and evaluating
112 them with surface observations in heavily dusty regions. We will then assess the relative contribution
113 of dust $PM_{2.5}$ to the global mortality and the overestimation of mortality resulting from defining dust
114 $PM_{2.5}$ with respect to the geometric size.

115 The rest of the paper is organized as follows. Section 2 describes the method used to estimate the
116 five-cause mortality attributable to long-term exposure to $PM_{2.5}$ and major datasets needed for the
117 calculation, including MERRA-2 $PM_{2.5}$ data. Section 3 presents an evaluation of MERRA-2 $PM_{2.5}$
118 against in-situ observations from the U.S. Diplomatic Posts around the world, the estimated $PM_{2.5}$-
119 attributable cause-specific and total mortalities, including its geopolitical distributions and respective
120 contributions by dust and non-dust (predominated by pollution) sources. This is followed by a
121 discussion in Section 4, including the need of distinguishing aerodynamic size from geometric size in
122 determining $PM_{2.5}$ from models and estimating the mortalities, the potential premature deaths
123 avoided if current $PM_{2.5}$-nonattainment areas were transformed to $PM_{2.5}$-attainment through a
124 hypothetical scenario of air pollution control, and major limitations of the study. Section 5
125 summarizes major conclusions of the study.

126

2 Description of data and methods

2.1 MERRA-2 aerosol reanalysis and surface $PM_{2.5}$

In this study, we use annual mean $PM_{2.5}$ concentrations simulated by MERRA-2 to determine the $PM_{2.5}$ exposure. MERRA-2 is a NASA meteorological and aerosol reanalysis for the modern satellite era (1979 - present) using the Goddard Earth Observing System model, version 5 (GEOS-5) (Gelaro et al., 2017). It runs at a nominal 50 km horizontal resolution with 72 vertical layers with the model top at ~85 km. In the GEOS-5 system, aerosols are simulated using a version of the Goddard Chemistry Aerosol Radiation and Transport (GOCART) model (Chin et al., 2002, 2009; Colarco et al., 2010). The GOCART simulates major components of aerosols, including sulfate, dust, black carbon, organic matter, and sea-salt. The model considers the atmospheric processes of chemistry, convection, advection, boundary layer mixing, dry and wet deposition, and gravitational settling (Chin et al., 2002; 2009). Aerosol particle sizes with a geometric diameter up to 20 μm are simulated with parameterized hygroscopic growth, which is a function of ambient relative humidity. Total mass of sulfate and carbonaceous aerosols are calculated, while for dust and sea salt the particle size distribution is explicitly resolved across five size bins (i.e., 0.2–2.0, 2.0–3.6, 3.6–6.0, 6.0-12.0, and 12.0-20.0 microns in the geometric diameter) (Chin et al., 2002). A log-normal distribution is assumed for mass in each size bin.

The assimilation of aerosols in MERRA-2 involves careful cloud screening and quality control (Zhang and Reid, 2006) and homogenization of the observing system by a Neural Net scheme (Lary et al., 2009) that translates satellite radiances (i.e., MODIS, MISR, AVHRR, and SeaWiFS) into aerosol optical depth (AOD). Observation and background errors are estimated using the maximum likelihood approach. Following the AOD analysis, 3D aerosol mass mixing ratio analysis increments are produced by exploring the Lagrangian characteristics of the aerosol distribution and generating local displacement ensembles intended to represent misplacements of the aerosol plumes (Buchard et al., 2017). Although the composition, size distribution, and vertical profile of aerosols are not assimilated in MERRA-2, previous evaluations have shown that the MERRA-2 aerosol assimilation system can also improve the surface $PM_{2.5}$ concentrations (Buchard et al., 2016) and specific aerosol components such as dust (Buchard et al., 2017; Randles et al., 2017).

In MERRA-2 products, surface $PM_{2.5}$ concentration by default is calculated as a sum of all aerosol components (sulfate, organic matter, black carbon, dust, and sea salt) with *geometric* diameter smaller than 2.5 μm, similar to the treatment of the GEOS-Chem model (http://wiki.seas.harvard.edu/geos-chem/index.php/Particulate_matter_in_GEOS-Chem#PM2.5_and_PM10_diagnostics_for_GEOS-Chem). We denote this MERRA-2 default $PM_{2.5}$ product as $PM_{2.5}^{geo}$ to distinguish it from the conventional definition of $PM_{2.5}$ based on the aerodynamic diameter in the air quality community. For sulfate and carbonaceous particles, they have a sub-micron size and $PM_{2.5}^{geo} = PM_{2.5}$. For dust particles covering a broad size range from submicron to super micron, dry mass in bin 1 (0.2 ~ 2.0 μm) and 38% of that in bin 2 (2.0 ~ 3.6 μm) are summed in diagnosing $PM_{2.5}^{geo}$ concentration. Clearly, this definition is inconsistent with the $PM_{2.5}$ in air quality and public health research communities. Many $PM_{2.5}$ in situ instruments are also designed to fractionate the size based on the aerodynamics. Kim et al. (2021) and Huang et al. (2021) emphasized the need of distinguishing aerodynamic size from geometric size when comparing different measurements or evaluating model simulations with measurements.

The aerodynamic diameter (D_{aer}) is the diameter of a sphere with a density close to water that has the same gravitational settling velocity as the dust particle with D_{geo}(Hinds, 1999). Given that the

dust particle (a density of about 2.6 g cm^{-3}) is much heavier than water by 160%, D_{aer} shall be larger than D_{geo}. Non-spherical shapes of dust particles also contribute to the difference between D_{aer} and D_{geo} because non-spherical particles fall at a slower rate than spherical particles do. Previous studies have shown that the D_{geo}/D_{aer} ratio generally falls into a range of 0.64 to 0.93 (e.g., Reid et al., 2003; Huang et al., 2021). In this study we use $\frac{D_{geo}}{D_{aer}} = 0.8$, similar to Kim et al. (2021). This means dust $PM_{2.5}$ (with D_{aer}≤2.5 μm) would have D_{geo}≤ 2.0 μm. Therefore, we use dust mass in the size-bin 1 (i.e., 0.2 ~ 2.0 μm) to approximate the dust $PM_{2.5}$, which is smaller than the default dust $PM_{2.5}^{geo}$ in MERRA-2 and GEOS-Chem diagnoses.

2.2 Mortality attributable to $PM_{2.5}$

We calculate cause-specific mortality attributable to long-term exposure of ambient $PM_{2.5}$ in the most current year (2019) for five diseases, namely ischaemic heart disease (IHD), cerebrovascular disease (CEV) or stroke, lung cancer (LC), chronic obstructive pulmonary disease (COPD), and acute lower respiratory infection (ALRI). We selected 2019, other than 2020 or 2021, to bypass complications arising from excess deaths associated with the COVID-19 pandemic. For each of the five causes (denoted by subscript i), the $PM_{2.5}$-attributable excess mortality ($\Delta Mort_i$) is calculated as:

$$\Delta Mort_i = b_i * pop * AF_i \quad (i=1, 2, \ldots\ldots, 5) \qquad (1)$$

where b_i is the baseline mortality rate for a specific cause, pop the population count, and AF_i the fraction of mortality attributable to exposure of $PM_{2.5}$. AF_i is further estimated from the relative risk (RR_i) or the concentration-response function (CRF) that describes how excess premature death increases with increasing $PM_{2.5}$ concentration, by following:

$$AF_i = \frac{RR_i - 1}{RR_i} \qquad (2)$$

For RR_i, we use CRFs based on the Integrated Exposure-Response (IER) model (Burnett et al., 2014), similar to that being used by the Global burden of disease (GBD) estimates and most studies in recent years (Lelieveld et al., 2015; Gannadaki et al., 2016; Cohen et al., 2017; Zhang et al., 2017). As shown in **Figure 1**, different diseases have different CRF. These CRFs are not always linear, depending on the range of $PM_{2.5}$ concentration. It is also worth noting that RR in Figure 1 remains at 1.0 (i.e., no impact on health) for $PM_{2.5}$ lower than 6-7 μg m^{-3}, depending slightly on the cause of mortality. This $PM_{2.5}$ level is considered as a threshold where $PM_{2.5}$ starts to pose a health risk, although there is an argument that no level of $PM_{2.5}$ is safe for human health. As discussed in Burnett et al. (2014), RRs show large spreads (see Figure S1 of supplement). We hence adopted their upper and lower bounds to represent the 95% confidence intervals (CI95) and then estimated the range of mortality at CI95. Like most other studies, we assume that all $PM_{2.5}$ components or sources have the same CRF. Although some studies suggested that mineral dust might be less toxic than sulfates and soot (Ozkaynak and Thurston, 1987; Ostro et al., 2010), this finding is not conclusive. It would be still reasonable to assume that there is no significant difference in the toxicity per unit mass of dust and anthropogenic pollution (Ostro et al., 2021).

We calculated cause-specific mortality attributable to the long-term exposure of ambient $PM_{2.5}$ in 2019 globally in 0.5°x 0.5°grid cells. Population count (pop) at the 0.5°x 0.5°grid cells were taken

from the Gridded Population of the World, Version 4 (GPWv4), Revision 11 provided by the NASA Socioeconomic Data and Applications Center (CIESN, 2018). We interpolated MERRA-2 $PM_{2.5}$ data into the 0.5°x 0.5° grid cells, consistent with the population data. The country-level baseline mortality rate b_i was acquired from the Institute for Health Metrics and Evaluation (IHME), Global Health Data Exchange (GHDx) (http://ghdx.healthdata.org/gbd-results-tool). For each grid, we determined the country and assigned the grid with the country-level b_i for 2019. The 2019 baseline mortality count, a product of baseline mortality rate and population, is shown in Figure S2 for individual causes. The geographical distribution of the mortality depends on cause of the death. The global total baseline mortality count is 2.45, 6.11, 3.26, 8.89, and 2.21 million for ALRI, CEV, COPD, IHD, and LC, respectively. The all-cause global total baseline mortality amounts to 22.73 million.

3. Results

In this section, we present an evaluation of MERRA-2 PM2.5 with data collected from a ground-based network, the estimated cause-specific mortality counts attributable to ambient $PM_{2.5}$ in 2019, and relative contributions from dust and pollution $PM_{2.5}$.

3.1. Spatial distribution of MERRA-2 $PM_{2.5}$ and its evaluation

Figure 2 shows a comparison of MERRA-2 annual $PM_{2.5}$ concentrations (defined by $D_{aer} \leq 2.5$ μm) (left panels) over global land with the MERRA-2 default output of $PM_{2.5}^{geo}$ (right panels) for both 2019 (top) and 2020 (bottom). Although $PM_{2.5}$ shows similar spatial patterns between 2019 and 2020, differences in the magnitude are evident in some regions. Notably, $PM_{2.5}$ in the American West was significantly higher in 2020 than 2019, presumably due to the record-breaking wildfires in 2020 (Williams et al., 2022). In both years, the $PM_{2.5}$ often exceeded 25 μg m^{-3} in the dust belt (North Africa and Middle East), India, and eastern China, implying a tremendous benefit of achieving the WHO AQG in these dusty and polluted regions. Clearly, $PM_{2.5}^{geo}$ (right panels) is significantly higher than $PM_{2.5}$ (left panel). This overestimate of $PM_{2.5}$ resulting from the use of geometric diameter is a factor of 2 or more in the dust belt and 10-30% in highly populated and polluted regions downwind of the dust sources. Therefore, the use of default $PM_{2.5}^{geo}$ output from MERRA-2 will lead to a significant overestimation of the mortalities in broad areas, which will be assessed in Section 4.2.

Overlaid on these MERRA-2 $PM_{2.5}$ and $PM_{2.5}^{geo}$ maps are annual average $PM_{2.5}$ (aerodynamic-size based) concentrations measured in the U.S. Diplomatic Posts (33 embassies/consulates in 2019 and 52 in 2020, where each station has $PM_{2.5}$ measurements in more than 270 days annually). Locations of these Diplomatic Posts and measured annual $PM_{2.5}$ concentrations are provided in the supplement (Table S1). These $PM_{2.5}$ observations are carried out by the U.S. State Department in collaboration with the U.S. Environmental Protection Agency (EPA), which adopts the EPA's protocol of instrument installation, operation, maintenance, and assurance of data quality for monitoring air quality in the U.S. The dataset is part of EPA AirNow Network. It appears that MERRA-2 agrees quite well with the surface observations in some stations while is biased low in others. Substantial differences stand out in Ulaanbaatar (Mongolia), Sarajevo (Bosnia), Kampala (Uganda), Antananarivo (Madagascar), and Lima (Peru), with MERRA-2 $PM_{2.5}$ and $PM_{2.5}^{geo}$ being lower than the observations by a factor of more than five. On the other hand, in the dust belt MERRA-2 $PM_{2.5}^{geo}$ is substantially higher than the surface observation, although MERRA-2 $PM_{2.5}$ agrees reasonably well with the station observation. **Figure 3** shows a detailed comparison of MERRA-2

$PM_{2.5}$ and $PM_{2.5}^{geo}$ with the in-situ $PM_{2.5}$ (>15 μg m^{-3}) in the heavily dusty U.S. Diplomatic Posts that are selected as ($PM_{2.5}^{geo}/PM_{2.5}$ ≥1.5 and $PM_{2.5}^{geo}$ - $PM_{2.5}$≥15 μg m^{-3}). In 16 of 17 heavily dusty U.S. Diplomatic Posts (except in Bamako of Mali, Figure 3), MERRA-2 $PM_{2.5}$ agrees with the in-situ observation within 35% (mean ± 1σ of 24 ± 7%, σ represents the standard deviation of bias). In comparison, MERRA-2 $PM_{2.5}^{geo}$ is 42% ~ 175% (100 ± 52%) higher than the in-situ $PM_{2.5}$ observation. Clearly the careful definition of $PM_{2.5}$ is essential for comparisons between model and observation and can greatly improve the exposure estimate in the dusty regions. To what extent the use of MERRA-2 $PM_{2.5}^{geo}$ would overestimate the mortality will be discussed in section 4.1.

For those less-dusty U.S. Diplomatic Posts (N=68), MERRA-2 $PM_{2.5}$ concentrations are mostly biased low. The average MERRA-2 to observed $PM_{2.5}$ ratio is 0.48, suggesting that the MERRA-2 $PM_{2.5}$ is about 2 times lower than the observation. China and India are the most polluted and populous countries and the $PM_{2.5}$-attributable mortality is expected to be the highest. **Figure 4** shows detailed comparisons of MERRA-2 $PM_{2.5}$ against the observations at nine U.S. Diplomatic Posts in China (Beijing, Guangzhou, Shanghai, and Shenyang) and India (Chennai, Hyderabad, Kolkata, Mumbai, and New Delhi), two countries that make up the majority of $PM_{2.5}$-attributable deaths (McDuffie et al., 2021; Cohen et al., 2017). In China, MERRA-2 performs quite well in Beijing and Guangzhou, with a bias (MERRA-2 to the observation ratio) of 0.75~1.08. In Shanghai, the bias is 0.81 in 2019 but 0.57 in 2020. In Shenyang of northeastern China, MERRA-2 $PM_{2.5}$ has a larger bias of 0.47 in both years, suggesting that MERRA-2 may underestimate in this region by a factor of about 2. In comparison, MERRA-2 performs more poorly in India. The bias ranges from 0.39 to 0.58, except that Chennai has a smaller bias of 0.71 in 2019. Given that the U.S. embassies and consulates are usually located in populous and heavily polluted urban areas, the MERRA-2's horizontal resolution of about 50 km may not be adequately fine to capture potentially high heterogeneity of $PM_{2.5}$ in urban areas. Thus, the underestimate of $PM_{2.5}$ by MERRA-2 would be lower than the biases discussed above, although a quantitative estimate of the low bias is not possible.

Figure 5 shows cumulative distribution functions (CDF) of population being exposed to annual concentrations of total $PM_{2.5}$ (blue solid line) and dust $PM_{2.5}$ (orange solid line) in 2019 based on MERRA-2 reanalysis. Clearly, 90.5% and 65.5% of global population were living in areas with annual $PM_{2.5}$ exceeding the WHO AQG of 5 μg m^{-3} and 10 μg m^{-3}, respectively. Even without any anthropogenic sources 29.2% and 15.0% of global population were still exposed to annual dust $PM_{2.5}$ concentration of >5 μg m^{-3} and >10 μg m^{-3}, respectively, suggesting significant health impacts imposed by dust and a grand challenge of abating air pollution problem through controlling anthropogenic emissions only. For comparison, we also show similar CDFs for population exposure to the MERRA-2 default total (blue dotted line) and dust (orange dotted line) $PM_{2.5}^{geo}$. Because $PM_{2.5}^{geo}$ is always higher than $PM_{2.5}$, a larger fraction of global population would live in areas with $PM_{2.5}^{geo}$ exceeding the WHO AQG. 98.7% and 46.0% of global population were exposed respectively to total and dust $PM_{2.5}^{geo}$ of >5 μg m^{-3} on an annual average basis. In this study we will quantify the mortality associated with the 2019 $PM_{2.5}$ level and how enforcing pollution control regulations globally to reach different targets could save lives.

3.2. Cause-specific mortalities due to total $PM_{2.5}$

We estimated the global total all-cause mortality attributable to total $PM_{2.5}$ at 2,889,578 or nearly 2.9 million a year, which is composed of 1,192,153 from IHD, 1,013,414 from CEV, 287,358 from COPD, 229,912 from ALRI, and 166,741 from LC. This suggests that 12.7% of 2019 baseline all-

cause mortality is attributed to total $PM_{2.5}$. The $PM_{2.5}$-attributable fraction is 9.4%, 16.6%, 8.8%, 13.4%, and 8.3% for ALRI, CEV, COPD, IHD, and LC, respectively, which is collectively determined by the spatial distributions of $PM_{2.5}$ (Figure 2a) and the baseline mortality count (Figure S2). The mortality is highly heterogeneous geographically, as shown in **Figure 6**. The cause-specific and all-cause mortality represents the number of deaths in each 0.5˚x 0.5˚ grid, for which the same color bar is used for all the panels. This is a combined effect of $PM_{2.5}$ level and population. with zero mortality in many areas. While mortality due to $PM_{2.5}$ is very low in many areas, the greatest mortality occurs in China and India, followed by West Africa, the western Europe, and the eastern U.S. Although $PM_{2.5}$ concentration in West Africa is higher than that in China and most of India (Figure 2a), the mortality in West Africa is significantly lower due mainly to the less population in West Africa. Pie charts in **Figure 7** show how global cause-specific and all-cause mortalities are distributed among countries, with top 10 ranked countries being distinguished by colors and the remaining countries being marked as "Other" in light gray. The top 10 countries account for 77-93% of the global total mortality, depending on the diseases. Among the top 10 countries, China is the largest contributor in all the diseases except ALRI, with the percent contribution ranging from 33% (IHD) to 69% (LC). For all-cause mortality, China is ranked as the largest contributor with a share of 43%. For ALRI, India surpasses China to become the largest contributor (33%). India is the second largest for the other four diseases (CEV, COPD, IHD, and LC), which yields a 23% share of global all-cause mortality due to $PM_{2.5}$. China and India combined account for about two thirds of global all-cause mortality. From the perspective of individual causes, the two countries constitute a majority (58-80%) of the mortality in all causes except ALRI. For ALRI, Nigeria has a mortality comparable to that of China.

How is our estimated all-cause mortality for 2019 compared with results in literature? The 2010 global mortality of 3.16 (CI95: 1.52 - 4.60) million by Giannadaki et al. (2016) and Lelieveld et al. (2015) agrees with our estimate of 2.89 (CI95: 1.38~4.48) millions within 10% (Table 1). Their estimated mortality of 1.31 million for CEV and 374 thousand for COPD is 30% higher than our corresponding estimates of 1.01 million and 287 thousand, which constitute the major difference between the two studies. For the other three causes (ALRI, IHD, and LC), the agreement is no more than 10%. In addition, the 2015 global mortality of 4.2 million estimated by Cohen et al. (2017) is about 45% higher than the 2.89 million estimated in this study. Zhang et al. (2017) estimated the global premature death of 3.45 million by using GEOS-Chem simulations of $PM_{2.5}$ to estimate the exposure, which is about 20% higher than our estimate. Burnett et al. (2018) developed a much higher RR based on the Global Exposure Mortality Model (GEMM) and estimated the global mortality of 8.9 (7.5-10.3) million in 2015, which is about a factor of 3 higher than our estimate. In summary, all these comparisons show that our estimated global all-cause mortality is smaller than previous estimates.

At the country-level, significant differences also exist among the studies. Table 2 compares our estimates of all-cause mortalities for top 10 countries with those from three studies (Cohen et al., 2017; Giannadaki et al., 2016; McDuffie et al., 2021). For example, Cohen et al. (2017) estimated mortalities in India, Russia, USA, and Bangladesh are substantially higher than those from the other studies. For China, Cohen et al. (2017) estimated its share in global mortality at 26%, which is lower than the 36-43% estimated by all the other studies. Clearly the ranking of top countries with high mortality differs among the studies. In addition, our estimate of total mortality of 1.23 million in China is consistent with the estimated 1.27 million deaths attributable to $PM_{2.5}$ in 2010 by Wang et al. (2017). For COPD, LC, IHD, and CEV, our respective estimates of mortality of 125, 114, 386, and 574 thousand in China are within 15% of that by Wang et al. (2017). On the other hand, our estimate of 33 thousand ALRI-related deaths is much higher than their estimated 4 thousand deaths.

Possible reasons for the differences in mortality among these studies include several aspects associated with $PM_{2.5}$ concentrations. However, pinpointing the differences between these studies needs substantial effort, which is beyond the scope of this study. $PM_{2.5}$ data sets used in these studies are for different years, i.e., 2010 for Lelieveld et al. (2015) and Giannadaki et al. (2016), 2015 for Cohen et al. (2017), and 2019 for this study. If significant trends have occurred in top 10 countries over the past decade, that would contribute to the mortality difference. The $PM_{2.5}$ datasets also have different spatial resolutions, ranging from 11 km (Cohen et al., 2017) to 0.5 deg (this study) and 1.1 deg (Lelieveld et al., 2015; Giannadaki et al., 2016). A higher resolution would generally yield a higher mortality, because of the correlation of high $PM_{2.5}$ level and dense population. These $PM_{2.5}$ datasets are also different in the extent to which the model simulations are constrained by observations. In Lelieveld et al. (2015) and Giannadaki et al. (2016), $PM_{2.5}$ concentrations are taken from simulations by a global chemical transport model. On the other hand, our study and Cohen et al. (2017) use $PM_{2.5}$ data that are constrained by satellite observations of AOD through data assimilation or data fusion. However, the $PM_{2.5}$ data used in Cohen et al. (2017) are defined by using the geometric size of particles, which will be higher than the aerodynamic-size defined $PM_{2.5}$ in this study, particularly in dust-dominated regions.

Differences in methods of calculating $PM_{2.5}$ exposure and mortality may also contribute to the differences in the estimated mortality shown in Table 1. Cohen et al. (2017) calculated the population-weighted mean $PM_{2.5}$ at country-level and then estimated the nation's mortality by using the CRF and baseline mortality data. The mortality was not calculated at 11km x 11km grid cells. This is different from our study, Lelieveld et al. (2015), and Giannadaki et al. (2016) where the mortality is calculated at grid cells first and then added up to obtain the country-level mortality. Given the non-linearity of the CRF, it is anticipated that the calculated mortalities from the two approaches might be different. We use the MERRA-2 $PM_{2.5}$ data and follow the method of Cohen et al. (2017) to calculate country-level mortality with the population-weighted country-level $PM_{2.5}$. For the global total, the so-estimated mortality of 2.63 million is only about 2.8% higher than our grid-level estimate of 2.56 million. On a regional scale the difference is slightly larger, for example with 6.1% in China and 4.5% in India.

3.3. Relative contributions by dust and pollution sources

We carry out a set of sensitivity tests to estimate relative contributions to the global mortality by $PM_{2.5}$ from dust storms versus non-dust sources. We consider $PM_{2.5}$ from all non-dust sources as a proxy for pollution $PM_{2.5}$, implying that biomass burning smoke and secondary organic aerosol formed from biogenic emissions are all counted as pollution aerosol. **Figure 8** shows spatial distributions of 2019 annual average pollution and dust $PM_{2.5}$ concentrations. The pollution $PM_{2.5}$ higher than 15 μg m^{-3} occurs in broad areas of East and South Asia and several hot spots presumably associated with fires in Siberia, Alaska (USA), Canada, and southern Africa. Not surprisingly, high dust $PM_{2.5}$ concentration occurs largely in the dust belt extending from North Africa to the western China, with the level greater than 50 μg m^{-3} in some major dust source regions.

We run the mortality calculation by using pollution $PM_{2.5}$ and then subtract it from the mortality by total $PM_{2.5}$ (shown in 3.2) to obtain the mortality attributable to dust $PM_{2.5}$. Similarly, another set of mortality is computed with dust $PM_{2.5}$ and the difference between the mortality attributable to total $PM_{2.5}$ and the mortality calculated with dust $PM_{2.5}$ is considered to represent the mortality attributable to pollution $PM_{2.5}$. Because of the nonlinearity of concentration-response functions (see Figure 1), the mortality attributable to dust $PM_{2.5}$ is about a factor of two higher that the mortality

388 computed with dust $PM_{2.5}$, while the mortality attributable to pollution $PM_{2.5}$ 17% higher that the
389 mortality computed with pollution $PM_{2.5}$. Table 3 compares respective contributions to the cause-
390 specific and all-cause global mortality being attributed to both pollution $PM_{2.5}$ and dust $PM_{2.5}$. On a
391 global average, the ratio of mortality attributable to dust $PM_{2.5}$ and pollution $PM_{2.5}$ ranges from 0.18
392 (LC) to 0.59 (ALRI), depending on the cause of mortality. For the all-cause mortality, the dust to
393 pollution ratio is 0.28. It is also necessary to note that due to the non-linear nature of the CRF
394 (Figure 1), adding up the so-derived mortalities attributed to pollution $PM_{2.5}$ and dust $PM_{2.5}$ yields an
395 all-cause mortality of 3.25 million, which is 13% larger than the baseline mortality by total $PM_{2.5}$.
396 Such high bias depends on the cause of mortality, ranging from 9% for IHD to 24% for ALRI.

397 Our estimated global all-cause mortality of 2.53 (1.21-3.86) million attributable to pollution $PM_{2.5}$ is
398 comparable to the 2.1 (1.3-3.0) millions by anthropogenic $PM_{2.5}$ in 2000 estimated from an ensemble
399 of chemistry-climate models (Silva et al., 2013). On the other hand, our estimated 721 (376-994)
400 thousand deaths attributable to dust $PM_{2.5}$ is 75% higher than the 412 thousand estimated by
401 Giannadaki et al. (2014) based on a global model simulation, presumably because dust $PM_{2.5}$ from
402 MERRA-2 reanalysis is higher than that simulated by the global aerosol model used in the latter
403 study. **Figure 9** shows spatial distributions of the calculated all-cause mortality attributed to pollution
404 $PM_{2.5}$ (a) and dust $PM_{2.5}$ (b), respectively. For the pollution $PM_{2.5}$, the mortality counts of more than
405 500 per 0.5x0.5 grid occur in highly populated eastern China and Indo-Gangetic plain. Large
406 mortality counts are also evident in other polluted regions such as West Europe and eastern US, and
407 Equatorial Africa. In comparison to the pollution-attributable mortality, the dust-attributable
408 mortality is generally lower in most of the regions except the areas adjacent to desert and with less
409 combustion sources such as West Africa and Middle East. In the highly populated Indian
410 subcontinent and the northern part of the eastern China, the dust-attributable mortality is similarly
411 high. Even in some parts of the western Europe and the eastern USA that are remote from the dust
412 source regions, dust can cause a significant number of deaths, due presumably to the intercontinental
413 transport of mineral dust (Yu et al., 2012, 2013b). Over uninhabited deserts, the very high $PM_{2.5}$
414 concentration (as shown in Figure 2a) yields zero exposure and zero mortality. To obtain a more
415 quantitative assessment of the relative role of pollution and dust $PM_{2.5}$, Table 4 compares pollution-
416 attributable and dust $PM_{2.5}$-attributable mortality in the top 10 countries. In Egypt and Nigeria, the
417 ratio of dust-attributable to pollution-attributable mortality is 3.86 and 1.95, respectively, suggesting
418 predominant role of dust in causing deaths due to their proximity to major dust sources in North
419 Africa and Middle East. Improving air quality in these countries depends strongly on how the wind-
420 erosion dust can be controlled. On the other hand, the dust to pollution mortality ratio is less than one
421 third in Indonesia, China, Bangladesh, Nepal, India, and the USA, suggesting the predominant
422 contributions of pollution $PM_{2.5}$ in these five countries. In particular, the dust contribution is
423 negligible in Indonesia, with a dust to pollution ratio of 0.03. For these countries, controlling
424 pollution emissions is an efficient pathway for improving air quality and reducing the death counts.
425 In between these two groups, the dust to pollution mortality ratio is 0.59 and 0.88 in Russia and
426 Pakistan, respectively, suggesting comparable roles of dust and pollution $PM_{2.5}$ in causing the excess
427 mortality.

428 Our estimate of dust $PM_{2.5}$-attributable mortality in this study is likely to be underestimated because
429 a substantially larger mass of dust particles coarser than 2.5 μm in aerodynamic diameter could cause
430 additional health issues such as asthma and other respiratory illnesses (Pope and Dockery, 2006;
431 Sandstrom and Forsberg, 2008). Dust plumes also carry a wide range of irritating spores, bacteria,
432 viruses, and persistent organic pollutants, posing significant health threats. The frequency of dust
433 storms in the southwestern US has been found to be strongly correlated with Valley fever incidences

(Tong et al., 2017). On top of the local dust, the long-range transport of dust plumes from North Africa and Asia may be a health concern for the U.S. (Schuerger et al., 2018).

4. Discussion

4.1. Overestimation of mortality resulting from using MERRA-2 $PM_{2.5}^{geo}$

Although it is widely known in the air quality and health community that $PM_{2.5}$ is defined based on the aerodynamic diameter, there exist some ambiguities in practical applications. Aerosol chemical transport models generally use geometric size to characterize the particle size distributions. As discussed in Section 2.1, some studies derive $PM_{2.5}^{geo}$ instead of $PM_{2.5}$ based on the aerodynamic size. The resulting overestimation of $PM_{2.5}^{geo}$ is particularly severe in the dust belt where dust particles are a predominating component of aerosol (see Figure 3). It is thus anticipated that the use of $PM_{2.5}^{geo}$ would significantly overestimate the mortality, with a magnitude depending on region and the cause of the mortality.

Here we quantify such overestimation by calculating the mortality with MERRA-2 $PM_{2.5}^{geo}$ in 2019 (Figure 2b) and then comparing the results with the baseline $PM_{2.5}$-attributable mortality (Section 3.2) calculated with MERRA-2 $PM_{2.5}$ (Figure 2a), as shown in Table 5 for cause-specific global mortalities. For COPD, IHD, LC, and CEV, the use of $PM_{2.5}^{geo}$ leads to an overestimation of mortality by 27-31%. For ALRI, however, the overestimation is as high as 60%, due to the predominance of ALRI in the dust belt (Figure 2a and Figure S2). For the all-cause mortality, the overestimation is about 1 million deaths or 32%. This exercise manifests the importance of distinguishing aerodynamic size from geometric size in defining $PM_{2.5}$ for assessing health outcomes resulting from $PM_{2.5}$ exposure. Reconciling the differences in estimated mortality in literature needs to factor in the difference in the definition of $PM_{2.5}$. It is also highly recommended that future studies define and report their $PM_{2.5}$ appropriately and clearly.

4.2. Potential health benefits of enforcing air pollution regulations to meet certain $PM_{2.5}$

To assess potential health benefits of enforcing air pollution regulations to meet the air quality standards related to $PM_{2.5}$, we carry out a set of idealized sensitivity tests by setting an upper limit of annual $PM_{2.5}$ concentration at a targeted level of 35, 25, 15, 10, and 5 μg m^{-3}, respectively. For grid cells with current $PM_{2.5}$ concentrations exceeding a targeted level (i.e., $PM_{2.5}$ nonattainment areas), we assign them with the targeted $PM_{2.5}$ level. For remaining grid cells, the $PM_{2.5}$ concentrations retain their current values. This scenario focuses on transforming grid cells from $PM_{2.5}$-nonattainment to $PM_{2.5}$-attainment, without accounting for continuous improvement of air quality in those already $PM_{2.5}$-attainment areas. These targeted $PM_{2.5}$ levels are selected based on a review of major ratified air quality standards or advocated guidelines around the world and are consistent with WHO's four interim target (IT) levels and AQG (Gannadaki et al., 2016; Chen and Hoek, 2020). The standard for annual $PM_{2.5}$ is set at 15 μg m^{-3} in the U.S. and several other countries, while the European Union targets at 25 μg m^{-3}. For comparison, China and India, two of the most polluted countries, are implementing a less stringent standard of 35 and 40 $\boldsymbol{\mu}$g/m3, respectively, in order to improve air quality and mitigate health impacts. WHO issued a guideline of 10 μg m^{-3} for annual $PM_{2.5}$ in 2005 and has recently updated it to 5 μg m^{-3} in 2021 (Chen and Hoek, 2020), which is the most stringent target of $PM_{2.5}$ control for mitigating adverse impacts on human health.

Figure 10 shows potential health benefits of enforcing air pollution regulations to transfer areas from $PM_{2.5}$ nonattainment to $PM_{2.5}$ attainment. Clearly, turning highly polluted areas to meet the 35 μg m^{-3} standard only yields an avoidance of 82 thousand premature deaths, which is 2.8% of $PM_{2.5}$-attributable global mortality. This suggests that highly polluted and populous regions like China, India and West Africa need to take more drastic actions to lower $PM_{2.5}$ concentration and protect the health of human beings in a meaningful way. A more stringent air quality standard should be adopted. With the implementation of more stringent $PM_{2.5}$ standards, potential health benefits out of the pollution controls would increase substantially. The avoided premature deaths from implementing the EU standard of 25 μg m^{-3} would increase to 383 thousand a year. If the U.S. AQS (15 μg m^{-3}) was successfully implemented globally, about 40% or 1.2 million of the $PM_{2.5}$-attributable deaths would be avoided, which represents a significant health benefit of the strict pollution control. If every place in the world is attainable to the old WHO guideline of 10 μg m^{-3}, the premature deaths avoided would increase to 1.85 million. The recent update of WHO $PM_{2.5}$ guideline from 10 to 5 μg m^{-3} would potentially save an additional one million lives a year.

There are caveats in the estimated health benefits under the simplified scenarios of pollution controls and regulations. On the one hand, potential health benefits of implementing air pollution control to meet the targeted air quality standards could be greater than that shown above, because $PM_{2.5}$ at a grid is kept the same when it is lower than the targeted standard. In the real world, even the pollution control strategy at local, regional, and national level may have much broader impacts in downwind regions because of the long-range transport of air pollution (Chin et al., 2007; Yu et al., 2008, 2012, 2013a, 2013b, 2015; Liu et al., 2009; Anenberg et al., 2014; Zhang et al., 2017). Note also that CRFs used in this study have a threshold of 6-7 μg m^{-3} for $PM_{2.5}$ starting to be harmful to human health. Therefore, our estimated health benefit here would represent a lower bound if such a threshold is lower or even does not exist.

On the other hand, $PM_{2.5}$ in the dust-dominated regions could be largely uncontrollable, because the dust emissions are driven by meteorological conditions (such as wind speed, soil moisture, vegetation covers, among others) that would be influenced by anthropogenic activities. When carving out the dust belt (17W-70E, 10N-35N) in calculating the health benefit, the global total health benefit would amount to 76, 356, 1090, 1708, and 2679 thousands for enforcing WHO IT and AQG of 35, 25, 15, 10, and 5 μg m^{-3}. This represents a 7% decrease in the full-scale health benefits reported in Figure 10.

Nevertheless, dust $PM_{2.5}$ might decrease in the future driven by climate change, leading to a health benefit. Observations have indicated that the dust emissions have been decreasing in recent decades in part of Gobi deserts and in the Middle East, due to the decades-long persistent effort of revegetation and irrigation expansion, respectively (Yu et al., 2020; Song et al., 2021; Xia et al., 2022). Yuan et al. (2020) identified based on distant and recent past dust records that the interhemispheric contrast of the Atlantic sea-surface temperature (SST) or ICAST has driven variability of African dust at decadal to millennial timescales. They further predicted that the increase of ICAST in the global warming scenarios would reduce African dust by more than 30% as early as 2050. If the decreasing trends of regional dust continue and the prediction of future dust decline is robust, the air quality in the dust belt would be improved in the future, leading to significant health benefits.

4.3. Major uncertainties associated with the mortality estimates

The estimated mortality in this study is subject to notable uncertainties associated with several sources. As discussed earlier, large spreads in the RR-$PM_{2.5}$ relationships as quantified by the 95%

confidence interval have led to the estimated global all-cause mortality ranging from 1.4 million to 4.5 million (i.e., a factor of more than 3 differences). A recent study (Burnett et al., 2018) suggests the IER RR could have been significantly underestimated, particularly at high $PM_{2.5}$ concentrations, suggesting that our estimate of global mortality may be biased low. Burnett et al. (2018) also suggested that there could be significant premature deaths that are not accounted for by the five diseases considered in this and other studies. In addition, the use of globally uniform RR-$PM_{2.5}$ relationship neglects its potentially large diversity from region to region. As a result, the estimated regional mortality has larger uncertainty than the global total mortality does. Tightening the range of estimated mortality requires that more cohort studies of health outcomes from $PM_{2.5}$ exposure be carried out in diverse regions.

The relatively coarse resolutions for $PM_{2.5}$, population, and the baseline mortality all contribute to the uncertainty in the estimated $PM_{2.5}$-attributable mortality. Given the co-existence of higher $PM_{2.5}$in more populous areas (e.g., urban areas), the use of coarse resolution $PM_{2.5}$ data would lead to an underestimate of the mortality. Improving model resolution is needed to resolve the heterogeneity of $PM_{2.5}$ concentrations in urban areas. Satellite pixel size has become finer, and some recent studies have taken advantage of this improvement to scale global chemical transport modeling of $PM_{2.5}$ at a relatively coarse resolution to as fine as 10 km on a global scale (Brauer et al., 2016) or even 1 km on a regional basis (Wei et al., 2021). Such high-resolution $PM_{2.5}$ data would be useful for future studies when a use of geometric size or aerodynamic size in defining $PM_{2.5}$is clarified, and associated bias is corrected. On the other note, the cause-specific total mortality rate is currently reported to WHO at country-level, which does not resolve sub-country variability. This can lead to large uncertainty in large country like China and Indian where many natural and social-economic factors can affect the mortality. However, it is unlikely that the spatial resolution of the mortality data could be significantly improved soon.

Although our evaluation shows very good agreement between MERRA-2 $PM_{2.5}$ and in situ observation in the heavily dusty regions, the MERRA-2 $PM_{2.5}$ on average is a factor of about 2 smaller than the in-situ measurements in other cities. Such low bias is heterogeneous in space. In China, MERRA-2 $PM_{2.5}$ agrees with the station measurement within 25% in eastern and southern China, the underestimate could reach a factor of 2 in northeastern China. Throughout India, MERRA-2 $PM_{2.5}$ is consistently smaller than the surface measurement by about a factor of 2. The low bias in the MERRA-2 $PM_{2.5}$ could be partially explained by the fact that the model's resolution is not fine enough to capture high heterogeneity of $PM_{2.5}$ in urban areas. We believe that even though MERRA-2 assimilates the satellite retrievals of AOD, it still underestimates $PM_{2.5}$ in non-dusty regions. Therefore, our estimated mortality in non-dusty regions is biased low. As a result, our estimate of dust fractional contribution to global mortality is likely biased high.

Using the same RR for all components of $PM_{2.5}$ assumes inherently that $PM_{2.5}$ has the same toxicity regardless of their sources (e.g., industrial pollution, biomass burning, and dust storms) and the toxicity depends only on the mass concentration of $PM_{2.5}$. This is like other studies in literature (e. g., Lelieveld et al., 2015; Giannadaki et al., 2016; Cohen et al., 2017; McDuffie et al., 2021). This oversimplification is made due to the lack of epidemiological studies for quantifying potential differences in the toxicity conclusively. It is challenging to isolate dust from a complex mixture of dust and anthropogenic aerosol and to measure the exposure to dust. Nevertheless, there is emerging evidence of dependence of toxicity on chemical composition or source of $PM_{2.5}$, though results are generally mixed (Ozkaynak and Thurston, 1987; Ostro et al., 2010, 2015; Thurston et al., 2016). Several papers have underscored the importance of and called for incorporating the chemical

composition or sources of $PM_{2.5}$ in the mortality assessment (Kinney et al., 2010; Lelieveld et al., 2015; West et al., 2016). Recently Chen et al. (2020) developed a component-adjusted approach to assess the joint impacts of $PM_{2.5}$ concentration and composition on mortality. It was found that accounting for the composition in the assessment could increase the cardiovascular mortality by 27% in a specific region. More research is warranted in the future to improve the quantitative understanding of chemical composition and sources of $PM_{2.5}$ on mortality to assess the health impacts of $PM_{2.5}$ more accurately. It also requires that $PM_{2.5}$ composition be observed in wide areas and simulated with chemical transport models with much improved accuracy, which poses a great challenge.

5. Conclusions

We estimated global premature deaths attributable to long-term exposure of ambient $PM_{2.5}$ in 2019 by using $PM_{2.5}$ from MERRA-2 aerosol reanalysis product and the cause-specific relative risks from the integrated exposure-response model. The estimated yearly global premature deaths attributable to ambient $PM_{2.5}$ exposure in 2019 amount to 2.89 (1.38 ~ 4.48) millions, which is composed of 1.19 (0.73 ~ 1.84) millions from IHD, 1.01 (0.35 ~ 1.55) millions from stroke, 0.29 (0.11 ~ 0.48) millions from COPD, 0.23 (0.14 ~ 0.33) millions from ALRI, and 0.17 (0.04 ~ 0.28) millions from LC. The mortality counts vary substantially with geopolitical regions, with the highest number of deaths occurring in Asia. China and India account for 43% and 23% of the global $PM_{2.5}$-attributable deaths, respectively. Although desert dust is emitted in remote and less populous regions, the dust plume can transport long distances and affects populations in downwind regions as far as different continents across oceans. The dust-attributable to pollution-attributable mortality ratio is 0.28 for all-cause deaths, suggesting that 22% of the global deaths are caused by desert dust. The relative contributions of dust and pollution sources vary with the causes of deaths (17-60%) and geographical regions.

We also assessed potential health benefits of enforcing air pollution regulations to transfer areas from $PM_{2.5}$ nonattainment to $PM_{2.5}$ attainment. The air quality standards currently being implemented in China and India, the two largest contributors of global mortality, do not yield a significant health benefit. More stringent air quality standards need to be enforced to produce significant health benefits. If every place in the world were attainable with the U.S. standard of 15 $\boldsymbol{\mu}$g/m^3, about 40% or 1.2 million of the $PM_{2.5}$-attributable deaths would have been avoided. Being attainable with the WHO guideline of 10 $\boldsymbol{\mu}$g/m^3 globally would have avoided 1.8 million or 64% of premature deaths. The most recent update of WHO $PM_{2.5}$ guideline from 10 to 5 $\boldsymbol{\mu}$g/m^3 would potentially save additional one million lives. These estimates would represent an underestimate of health benefit if the regions around the world currently in compliance with the AQS continue to improve the air quality.

Our study manifests the importance of distinguishing aerodynamic size from geometric size in validating simulated $PM_{2.5}$ concentrations and accurately assessing their global health burden. A use of geometric size in diagnosing dust $PM_{2.5}$ from the model simulation could significantly overestimate the $PM_{2.5}$ level in the dust belt by 40-170%, leading to an overestimate of global all-cause mortality by 1 million deaths or 32%. We recommend that the aerosol modeling community clarify the existing ambiguity on defining the $PM_{2.5}$.

Despite a reasonably good agreement with other estimates of global mortality, our estimates are subject to significant uncertainties, including low bias in the MERRA-2 $PM_{2.5}$ in highly polluted cities, large spread in the concentration-response functions (CRF), and the negligence of potential CRF regional variability and sub-country variability in the baseline mortality rate. Our calculation also assumes that $PM_{2.5}$ from different sources have the same toxicity, which may not hold true as

suggested by a few lines of emerging evidence. Reducing these uncertainties requires substantial, cross-disciplinary efforts on improving the estimate of $PM_{2.5}$ exposure and establishing more rigorous CRF accounting for the dependencies on geopolitical regions and $PM_{2.5}$ sources through epidemiological cohort studies.

Conflict of Interest

The authors declare that the research was conducted in the absence of any commercial or financial relationships that could be construed as a potential conflict of interest.

Author Contributions

HY: conceptualization, methodology, formal analysis, investigation, writing—original draft, visualization, and project administration. AY: methodology, mortality calculations, formal analysis, investigation, visualization, and contributing to the writing of original draft; QT: processing ground-based $PM_{2.5}$ data, and visualization; CR: processing MERRA-2 $PM_{2.5}$ data and formatting baseline mortality and IER CRF data; MC: conceptualization. All authors contributed to reviewing and editing of the article and approved the submitted version.

Acknowledgments

AY was supported by the National Space Club Fellowship program for his work during the summer of 2021 at NASA Goddard Space Flight Center. Other co-authors are supported by different NASA earth science research programs including the Modeling, Analysis, and Prediction (MAP) program and the Atmospheric Composition Modeling and Analysis Program (ACMAP). We are grateful to Dr. Virginie Buchard for providing insights into the calculation of $PM_{2.5}$ in MERRA-2, and Dr. Fei Liu and Dr. Qing Liu for their help on providing tools to downscale country-based data into the model grids.

Data availability

The data used in this study for estimating global health burden attributable to $\mathbf{PM_{2.5}}$ were downloaded from a range of sources. Population data, the Gridded Population of the World, Version 4 (GPWv4), Revision 11, were downloaded from the NASA Socioeconomic Data and Applications Center (https://sedac.ciesin.columbia.edu/data/collection/gpw-v4/sets/browse). The country-level baseline mortality rate was acquired from the Institute for Health Metrics and Evaluation (IHME), Global Health Data Exchange (GHDx) (http://ghdx.healthdata.org/gbd-results-tool). The IER-based CRFs were downloaded from https://ghdx.healthdata.org/record/ihme-data/gbd-2010-ambient-air-pollution-risk-model-1990-2010. MERRA-2 data were downloaded from MDISC at https://disc.gsfc.nasa.gov/datasets?project=MERRA-2, managed by the NASA Goddard Earth Sciences (GES) Data and Information Services Center (DISC). Surface $\mathbf{PM_{2.5}}$ observations in the

U.S. Diplomatic Posts were downloaded from https://www.airnow.gov/international/us-embassies-and-consulates/.

References:

Anenberg, S., West, J. J., Yu, H., Chin, M., Schulz, M., Bergmann, D., Bey, I., Bian H., Diehl, T., Fiore, A., Hess, P., Marmer, E., Montanaru, V., Park, R., Shindell, D., Takemura, T., Dentener, F., Impacts of intercontinental transport of anthropogenic fine particulate matter on human mortality, Air Qual. Atmos. Health, doi:10.1007/s11869-014-0248-9, 2014.

Bauer, S., Im, U., Mezuman, K., Gao, C. Y., Desert dust, industrialization, and agricultural fires: Health impacts of outdoor air pollution in Africa, J. Geophys. Res. - Atmos., 124, 4104-4120, https://doi.org/10.1029/2018JD029336, 2019.

Brauer, M., et al., Ambient air pollution exposure estimation for the global burden of disease 2013, Environ. Sci. Technol., 50, 79-88, doi:10.1021/acs.est.5b03709, 2016.

Buchard, V., Randles, C. A., Da Silva, A. M., Darmenov, A., Colarco, P. R., Govindaraju, R., Ferrare, R., Hair, J., Beyersdorf, A. J., Ziemba, L. D., and Yu, H., The MERRA-2 aerosol reanalysis, 1980 onward. Part II: Evaluation and case studies, J. Climate, 30, 6851- 6872, 2017.

Buchard, V., da Silva, A. M., Randles, C. A., Colarco, P. R., Ferrare, R., Hair, J., Hostetler, C., Tackett, J., and Winker, D., Evaluation of the surface PM2.5 in Version 1 of the NASA MERRA Aerosol Reanalysis over the United States, Atmos. Environ., 125, 100-111, 2016.

Burnett, R. T., et al., An integrated risk function for estimating the global burden of disease attributable to ambient fine particulate matter exposure, Environ. Health Perspectives, 122, http://dx.doi.org/10.1289/ehp.1307049, 2014.

Burnett, R. T., et al., Global estimates of mortality associated with long-term exposure to outdoor fine particulate matter, Proc. Natl. Acad. Sci. USA, 115, 9592-9597, 2018.

Chen, H., Zhang, Z., van Donkelaar, A., Bai, L., Martin, R. V., Lavigne, E., Kwong, J. C., and Burnett, R. T., Understanding the joint impacts of fine particulate matter concentration and composition on the incidence and mortality of cardiovascular disease: A component-adjusted approach, Environ. Sci. Technol., 54, 4388-4399, https://dx.doi.org/10.1021/acs.est.9b06861, 2020.

Chen, J., and Hoek, G., Long-term exposure to PM and all-cause and cause-specific mortality: A systematic review and meta-analysis, Environ. International, 143, 105974, http://doi.org/10.1016/j.envint.2020.105974, 2020.

Chin, M., Ginoux, P., Kinne, S., Torres, O., Holben, B. N., Duncan, B. N., Martin, R. V., Logan, J. A., Higurashi, A., and Nakajima, T., Tropospheric aerosol optical thickness from the GOCART model and comparisons with satellite and sun photometer measurements, J. Atmos. Sci., 59, 461-483, 2002.

Chin, M., Diehl, T., Ginoux, P., and Malm, W. Intercontinental transport of pollution and dust aerosols: implications for regional air quality. Atmos. Chem. Phys., 7, 5501-5517, 2007.

Chin, M., Diehl, T., Dubovik, O., Eck, T. F., Holben, B. N., Sinyuk, A., and Streets, D. Light absorption by pollution, dust, and biomass burning aerosols: a global model study and evaluation with AERONET measurements. Ann. Geophys., 27, 3439-3464, www.ann-geophys.net/27/3439/2009/, 2009

CIESIN (Center for International Earth Science Information Network) - Columbia University. 2018. Gridded Population of the World, Version 4 (GPWv4): Population Count, Revision 11. Palisades, NY: NASA Socioeconomic Data and Applications Center (SEDAC). https://doi.org/10.7927/H4JW8BX5. Accessed 20 August, 2021.

Cohen, A. J., et al., Estimates and 25-year trends of the global burden of disease attributable to ambient air pollution: an analysis of data from the Global Burden of Disease Study 2015, Lancet, 389:1907-1918, http:/dx.doi.org/10.1016/s0140-6736(17)30505-6, 2017.

Colarco, P., daSilva, A., Chin, M., and Diehl, T. Online simulations of global aerosol distributions in the NASA GEOS-4 model and comparisons to satellite and ground-based aerosol optical depth. J. Geophys. Res., 115 (D14): D14207, doi :10.1029/2009JD012820, 2010.

De Longueville, F., Ozer, P., Doumbia, S., and Henry S., Desert dust impacts on human health: an alarming worldwide reality and a need for studies in West Africa, Int. J. Biometeorol., 57, 1-19, doi:10.1007/s00484-012-0541-y, 2013.

Evans, J., van Donkelaar, A., Martin, R. V., Burnett, R., Rainham, D. G., Birkett, N. J., and Krewski, D., Estimates of global mortality attributable to particulate air pollution using satellite imagery, Environ. Res., 120, 33-42, 2013.

GBD 2019 Risk Factor Collaborators. Global burden of 87 risk factors in 204 countries and territories, 1990–2019: a systematic analysis for the Global Burden of Disease Study 2019. Lancet, 396, 1223–1249, 2020.

Gelaro, R., W. McCarty, M. J. Suárez, R. Todling, A. Molod, L. Takacs, C. Randles, A. Darmenov, M. G. Bosilovich, R. Reichle, K. Wargan, L. Coy, R. Cullather, C. Draper, S. Akella, V. Buchard, A. Conaty, A. da Silva, W. Gu, G.-K. Kim, R. Koster, R. Lucchesi, D. Merkova, J. E. Nielsen, G. Partyka, S. Pawson, W. Putman, M. Rienecker, S. D. Schubert, M. Sienkiewicz, and B. Zhao. The Modern-Era Retrospective Analysis for Research and Applications, Version 2 (MERRA-2). J. Climate. 30: 5419–5454, 2017.

Giannadaki, D., Pozzer, A., & Lelieveld, J., Modeled global effects of airborne desert dust on air quality and premature mortality. Atmos. Chem. Phys., 14(2), 957-968, 2014,

Ginnadaki, D., Lelieveld, J., and Pozzer, A., Implementing the US air quality standard for PM2.5 worldwide can prevent millions of premature deaths per year, Environ. Health, 15:88, doi:10.1186/s12940-016-0170-8, 2016.

Ginoux, P., Chin, M., Tegen, I., Prospero, J. M., Holben, B. N., Dubovik, O., and Lin, S.-J., Sources and distributions of dust aerosols simulated with the GOCART model, J. Geophys. Res., 106, 20255-20273, 2001.

718 Glinianaia, S. V., Rankin, J., Bell, R., Pless-Mulloli, T., and Howel, D., Particulate air pollution and
719 fetal health: a systematic review of the epidemiological evidence, Epidemiology, 15, 36-45, 2004.

720 Heft-Neal, S., Burney, J., Bendavid, E., Voss, K. K., and Burke, M., Dust pollution from the Sahara
721 and African infant mortality, Nature Sustainability, 3 (10), 863-871, 2020.

722 Hinds, W. C., Aerosol technology: properties, behavior, and measurement of airborne particles (2nd
723 ed,), Wiley-Interscience.

724 Huang, Y., Adebiyi, A. A., Formenti, P., and Kok, J. F., Linking the different diameter types of
725 aspherical desert dust indicates that most models underestimate coarse dust emission, Geophys. Res.
726 Lett., 48, e2020GL092054, https://doi.org/10.1029/2020GL092054, 2021.

727 Huneeus, N., et al., Global dust model intercomparison in AeroCom phase I., Atmos. Chem. Phys.,
728 11(15), 7781-7816, 2011.

729 Karanasiou, A., N. Moreno, T. Moreno, M. Viana, F. de Leeuw, and X. Querol. Health effects from
730 Sahara dust episodes in Europe: Literature review and research gaps. Environ. International, 47:107–
731 14, 2012.

732 Kim, D., Chin, M., Cruz, C. A., Tong, D., and Yu, H. Spring dust in western North America and its
733 interannual variability—Understanding the role of local and transported dust. J. Geophys. Res. -
734 Atmos., 126 (22), doi: 10.1029/2021jd035383, 2021.

735 Kinney, P. L., et al., On the use of expert judgment to characterize uncertainties in the health benefits
736 of regulatory controls of particulate matter, Environ. Sci. Policy, 13, 434-443, 2010.

737 Lary, D., Remer, L. A., MacNeill, D., Roscoe, B., and Paradise, S. Machine learning and bias
738 correction of MODIS aerosol optical depth. IEEE Geosci. Remote Sensing Lett. 6 (4): 694-698
739 [10.1109/LGRS.2009.2023605], 2009.

740 Lelieveld, J., Evans, J. S., Fnais, M., Giannadaki, D., Pozzer, A., The contribution of outdoor air
741 pollution sources to premature mortality on a global scale, Nature, 525, 367-371,
742 doi:10.1038/nature15371, 2015.

743 Lim, S. S., Vos, T., Flaxman, A. D., Danaei, G., Shibuya, K., Adair-Rohani, H., A Comparative Risk
744 Assessment of Burden of Disease and Injury Attributable to 67 Risk Factors and Risk Factor Clusters
745 in 21 Regions, 1990-2010: A Systematic Analysis for the Global Burden of Disease Study 2010.
746 Lancet 380 (9859): 2224–2260, 2012.

747 Liu, J., Mauzerall, D. L., andHorowitz, L. W., Evaluating inter-continental transport of fine aerosols:
748 (2) Global health impact, Atmos. Environ., 43, 4339-4347, 2009.

749 McDuffe, E. E., Martin, R. V., Spadaro, J. V., Burnett, R., Smith, S. J., O'Rourke, P., et al., Source
750 sector and fuel combustions to ambient PM2.5 and attributable mortality across multiple spatial
751 scales, Nat. Commun., 12, 3594, doi:10.1038/s41467-021-23853-y, 2021.

752 Ostro, B., Lipsett, M., Reynolds, P., Goldberg, D., Hertz, A., Garcia, C., Henderson, K. D.,
753 Bernstein, L., Long-term exposure to constituents of fine particulate air pollution and mortality:
754 results from the California teachers study, Environ. Health Perspective, 118, 363-369, 2010.

Ostro, B., Hu, J., Goldberg, D., Reynolds, P., Hertz, A., Bernstein, L., and Kleeman, M. J., Associations of mortality with long-term exposure to fine and ultrafine particles, species and sources: Results from the California teachers study cohort, Envion. Health Perspective, 123, 549-556, http://dx.doi.org/10.289/ehp.1408565, 2015.

Ostro, B., Awe, B., and Sanchez-Triana, E., When the dust settles: A review of the health implications of the dust component of air pollution, 75pp, Pollution Management & Environmental Health, World Bank Group, Washington DC, 2021.

Pai, S. J., Carter, T. S., Heald, C. L., and Kroll, J. H., Updated World Health Organization Air Quality Guidelines highlight the importance of non-anthropogenic $PM_{2.5}$, Environ. Sci. Technol. Lett., 9, 501-506, 2022.

Pope, C. A., et al., Lung cancer, cardiopulmonary mortality, and long-term exposure to fine particulate air pollution, JAMA, 287, 1132-1141, 2002.

Pope III, C. A. and Dockery, D. W., Critical review health effects of fine particulate air pollution: lines that connect, J. Air Waste Manag. Assoc., 56, 709-742, 2006.

Power, M.C., Adar, S. D., Yanosky, J. D., Weuve, J., Exposure to air pollution as a potential contributor to cognitive function, cognitive decline, brain imaging, and dementia: A systematic review of epidemiologic research, Neurotoxicology, 56, 235-253, doi:10.1016/j.neuro.2016.06.004, 2016.

Randles, C. A., A. M. da Silva, V. Buchard, P. R. Colarco, A. Darmenov, R. Govindaraju, A. Smirnov, B. Holben, R. Ferrare, J. Hair, Y. Shinozuka, and C. J. Flynn. The MERRA-2 Aerosol Reanalysis, 1980 – onward, Part I: System Description and Data Assimilation Evaluation. J. Climate. 30 (17): 6823-6850 [10.1175/jcli-d-16-0609.1], 2017.

Reid, J. S., Johnson, H. H., Maring, H. B., Smirnov, A., Savoie, A. L., Cliff, S. S., et al., Comparison of size and morphological measurements of coarse mode dust particles from Africa. J. Geophys. Res. Atmos. 108(D19), 8593. https://doi.org/10.1029/2002JD002485, 2013.

Sandstrom, T., & Forsberg, B., Desert dust: an unrecognized source of dangerous air pollution? Epidemiology, 19(6), 808-809, 2008.

Schraufnagel, D. E., et al., Air pollution and noncommunicable diseases: Review by the Forum of International Respiratory Societies' Environmental Committee, Part 1: The Damaging Effects of Air Pollution, Chest, 155, 409-416, 2019.

Schuerger, A. C., Smith, D. J., Griffin, D. W., Jaffe, D. A., Wawrik, B., Burrows, S. M., ... & Yu, H., Science questions and knowledge gaps to study microbial transport and survival in Asian and African dust plumes reaching North America. Aerobiologia, 34(4), 425-435, 2018

Shaddick, G., Thomas, M. L., Mudu, P., Ruggeri, G., and Gumy, S., Half the world's population are exposed to increasing air pollution. NPJ Climate and Atmospheric Science, 3:23, https://doi.org/10.1038/s41612-020-0124-2, 2020.

Silva, A., et al., Global premature mortality due to anthropogenic outdoor air pollution and the contribution of past climate change, Environ. Res. Lett., 8, 034005, doi:10.1088/1748-9326/8/3/034005, 2013.

Song, Q., Zhang, Z., Yu, H., Ginoux, P., and Shen, J., Global dust optical depth climatology derived from CALIOP and MODIS aerosol retrievals on decadal timescales: regional and interannual variability, Atmos. Chem. Phys., 21, 13369-13395, 2021.

Stafoggia, M., Samoli, E., Alessandrini, E., Cadum, E., Ostro, B., Berti, G., ... & Med-Particles Study Group. Short-term associations between fine and coarse particulate matter and hospitalizations in Southern Europe: results from the MED-PARTICLES project. Environmental Health Perspectives, 121(9), 1026-1033, 2013.

Stafoggia, M., Zauli-Sajani, S., Pey, J., Samoli, E., Alessandrini, E., Basagaña, X., ... & MED-particles study group, Desert dust outbreaks in Southern Europe: contribution to daily PM_{10} concentrations and short-term associations with mortality and hospital admissions. Environmental Health Perspectives, 124(4), 413-419, 2016.

Thurston, George D., Kazuhiko Ito, Ramona Lall, Richard T. Burnett, Michelle C. Turner, Daniel Krewski, Yuanli Shi, Michael Jerrett, Susan M. Gapstur, W. Ryan Diver, and C. Arden Pope III. NPACT Study 4. Mortality and Long-Term Exposure to $PM_{2.5}$ and Its Components in the American Cancer Society's Cancer Prevention Study II Cohort. National Particle Component Toxicity (NPACT) Initiative: Integrated Epidemiologic and Toxicologic Studies of the Health Effects of Particulate Matter Components. Research Report 177. Boston, MA: Health Effects Institute, 2013.

Thurston, G. D., Burnett, R. T., Turner, M. C., Shi, Y., Krewski, D., Lall, R., Ito, K., Jerrett, M., Gapstur, S. M., Diver, W. R., and Pope, C. A. III, Ischemic heart disease mortality and long-term exposure to source-related components of U.S. fine particle air pollution, Environ. Health Perspect, 124, 785-794, http://dx.dot.org/10.1289/ehp.1509777, 2016.

Tong, D. Q., Wang, J. X., Gill, T. E., Lei, H., & Wang, B., Intensified dust storm activity and Valley fever infection in the southwestern United States. Geophys. Res. Lett., 44(9), 4304-4312, 2017.

Wang, Q., Wang, J., He, M. Z., Kinney, P. L., and Li, T., A county-level estimate of $PM_{2.5}$ related chronic mortality risk in China based on multi-model exposure data, Environ. Int., 110, 105-112, doi:10.1016/j.envint.2017.10.015, 2017.

Wei, J., Li, Z., Lyapustin, A., Sun, L., Peng, Y., Xue, W., Su, T., and Cribb, M. Reconstructing 1-km-resolution high-quality $PM_{2.5}$ data records from 2000 to 2018 in China: spatiotemporal variations and policy implications. Remote Sens. Environ., 252, 112136. https://doi.org/10.1016/j.rse.2020.112136, 2021.

West, J. J., et al., What we breathe impacts our health: Improving understanding of the link between air pollution and health, Environ. Sci. Technol., 50, 4895-4904, doi:10.1021/acs.est.5b03827, 2016.

Williams, A. P., Livnehg, B., McKinnon, K. A., Hansen, W. D., Mankin, J. S., Cook, B. I., Smerdon, J. E., Varuolo-Clarke, A., Bjarke, N. R., Juang, C. S., and Lettenmaier, D. P., Growing impact of wildfire on western US water supply, Proc. Natl. Acad. Sci. USA, 119, e2114069119, https://doi.org/10.1073/pnas.2114069119, 2022.

Xia, W., Wang, Y., & Wang, B, Decreasing dust over the Middle East partly caused by irrigation expansion. Earth's Future, 10, e2021EF002252, https://doi.org/10.1029/2021EF002252, 2022.

Yu, H., Remer, L. A., Chin, M., Bian, H., Kleidman, R. G., and Diehl, T., A satellite-based assessment of transpacific transport of pollution aerosol, J. Geophys. Res. -Atmos., 113, D14S12, doi:10.1029/2007JD009349, 2008.

Yu, H., Remer, L. A., Chin, M., Bian, H., Tan, Q., Yuan, T., and Zhang, Y., Aerosols from overseas rival domestic emissions over North America, Science, 337, 566-569, 2012.

Yu, H., M. Chin, J. West, C. Atherton, N. Bellouin, I. Bey, D. Bergmann, H. Bian, T. L. Diehl, G. Forberth, P. Hess, M. Schulz, D. T. Shindell, T. Takemura, and Q. Tan. A multimodel assessment of the influence of regional anthropogenic emission reductions on aerosol direct radiative forcing and the role of intercontinental transport, J. Geophys. Res. - Atmos., 118, 700-720, doi:10.1029/20212JD0180148, 2013a.

Yu, H., L. A. Remer, R. A. Kahn, M. Chin, and Y. Zhang. Satellite perspective of aerosol intercontinental transport: From qualitative tracking to quantitative characterization. Atmos. Res. 124 73-100, doi:10.1016/j.atmosres.2012.12.013, 2013b.

Yu, H., Chin, M., Yuan, T., Bian, H., Remer, L. A., Prospero, J. M., Omar, A., Winker, D., Yang, Y., Zhang, Y., Zhang, Z., and Zhao, C., The fertilizing role of African dust in the Amazon rainforest: A first multiyear assessment based on data from Cloud-Aerosol Lidar and Infrared Pathfinder Satellite Observations, Geophys. Res. Lett., 42, doi:10.1002/2015GL063040, 2015.

Yu, H., Yang, Y., Wang, H., Tan, Q., Chin, M., Levy, L.C., Remer, L.A., Smith, S. J., Yuan, T., and Shi, Y., Interannual variability and trends of combustion aerosol and dust in major continental outflows revealed by MODIS retrievals and CAM5 simulations during 2003-2017, Atmos. Chem. Phys., 20, 139-161, 2020.

Yuan, T., Yu, H., Chin, M., Remer, L. A., McGee, D., and Evan, A., Anthropogenic decline of African dust: Insights from the Holocene records and beyond. Geophys. Res. Lett., 47, e2020GL089711. https://doi.org/10.1029/2020GL089711, 2020.

Zhang, J., and Reid, J. S., MODIS aerosol product analysis for data assimilation: Assessment of over-ocean level 2 aerosol optical thickness retrievals, J. Geophys. Res., 111, D22207, doi:10.1029/2005JD006898, 2006.

Zhang, Q., et al., Transboundary health impacts of transported global air pollution and international trade, Nature, 543, 705-709, doi:10.1038/nature21712, 2017.

861 **Tables**

862

Table 1: Estimated global premature mortality (thousands) attributable to long-term exposure of ambient $PM_{2.5}$ in 2019 based on median RR and its CI95 range. Giannadaki et al. (2016) estimated mortality for 2010 is listed for comparison.

Cause	This study median mortality count (CI95)	Giannadaki et al. (2016)
ALRI	230 (141-332)	230
COPD	287 (114-477)	374
IHD	1192 (730-1840)	1080
LC	167 (37-276)	161
CEV	1013 (354-1554)	1310
All-cause	2890 (1376-4479)	3155 (1520-4600)

863

864

865

866

Table 2: Comparison of the estimated 2019 all-cause mortality (worldwide and the top 10 ranked countries) from this study with that of three studies (McDuffie et al., 2021; Cohen et al., 2017; Gannadaki et al., 2016). The mortality has a unit of thousand persons. For individual countries, the number in parentheses represents the percentage of a country contributing to the global total mortality.

Geopolitical region	this study for 2019	McDuffie et al. (2021) for 2017	Cohen et al. (2017) for 2015	Giannadaki et al., (2016) for 2010
World	2890 (CI95: 1376 - 4479)	3833 (CI95: 2720 - 4970)	4241	3155 (CI95: 1520 - 4600)
China	1232 (43%)	1387 (36%)	1108 (26%)	1327 (42%)
India	676 (23%)	867 (23%)	1090 (25%)	575 (18%)
Pakistan	86 (3.0%)	86 (2.2%)	135 (3.2%)	105 (3.3%)
Bangladesh	86 (3.0%)	64 (1.7%)	122 (2.9%)	85 (2.7%)
Nigeria	62 (2.1%)	51 (1.3%)	51 (1.2%)	89 (2.8%)
Indonesia	54 (1.9%)	94 (2.5%)	79 (1.9%)	51 (1.6%)
Russia	52 (1.8%)	68 (1.8%)	137 (3.2%)	67 (2.1%)
Egypt	43 (1.5%)	88 (2.3%)	*n/a*	34 (1.1%)
USA	39 (1.3%)	47 (1.2%)	88 (2.1%)	52 (1.7%)
Nepal	34 (1.2%)	*n/a*	*n/a*	*n/a*

867
868
869

870
871

Table 3: Estimated cause-specific and all-cause global mortality (unit: thousands) attributable respectively to dust and pollution $PM_{2.5}$ in 2019 based on median RR and its CI95 range.			
Cause	Pollution-attributable $\Delta Mort$	Dust-attributable $\Delta Mort$	Dust: Pollution
ALRI	179 (115-247)	106 (72-136)	0.59
CEV	937 (327-1416)	223 (74-306)	0.24
COPD	265 (108-426)	54 (25-80)	0.20
IHD	994 623-1512)	309 (199-428)	0.31
LC	158 (35-261)	28 (7-44)	0.18
All-cause	2532 (1209-3861)	721 (376-994)	0.28

872
873
874

875

Table 4: Pollution-attributable and dust-attributable mortality (thousands) in the top 10 countries

Country	Pollution-attributable $\Delta Mort$	Dust-attributable $\Delta Mort$	Dust: Pollution
China	1215	104	0.09
India	588	135	0.23
Pakistan	44	39	0.88
Bangladesh	86	10	0.11
Nigeria	25	49	1.95
Indonesia	54	2	0.03
Russia	52	28	0.54
Egypt	11	41	3.68
USA	39	13	0.33
Nepal	31	6	0.20

876
877

878
879

Table 5: Comparison of estimated global cause-specific deaths (thousands) attributable to long-term exposure of ambient $PM_{2.5}$ in 2019 between using $PM_{2.5}$ (Figure 2A) and $PM_{2.5}^{geo}$ (Figure 2B).			
Cause	with MERRA-2 $PM_{2.5}$	with MERRA-2 $PM_{2.5}^{geo}$	mortality ratio ($PM_{2.5}^{geo}$:$PM_{2.5}$)
ALRI	228	368	1.60
CEV	1013	1326	1.31
COPD	287	366	1.27
IHD	1192	1543	1.29
LC	167	219	1.31
all-cause	2890	3822	1.32

880

881

Figure captions:

Figure 1: Relative risk (RR) as a function of $PM_{2.5}$ concentration (μg m^{-3}) or concentration-response function (CRF) for individual causes of mortality, including ALRI, COPD, IHD, LC, and CEV.

Figure 2: Annual average $PM_{2.5}$ (left panels) and $PM_{2.5}^{geo}$ (right panels) concentrations (μg m^{-3}) from MERRA-2 reanalysis in 2019 (a and b) and 2020 (c and d). $PM_{2.5}$ concentrations measured in the U.S. Diplomatic Posts (greater than 270 days in a year) are overlaid on the MERRA-2 $PM_{2.5}$ maps with the same color scale.

Figure 3: Comparisons of observed $PM_{2.5}$ (black) and MERRA-2 $PM_{2.5}$ (orange) and $PM_{2.5}^{geo}$ (blue) in the heavily dusty U.S. Diplomatic Posts as defined in the text. $PM_{2.5}$ has a unit of μg m^{-3}.

Figure 4: Comparisons of MERRA-2 $PM_{2.5}$ concentration (μg m^{-3}) in 2019 and 2020 with the observations at nine U.S. Diplomatic Posts in China and India.

Figure 5: Cumulative distribution functions (CDFs) of population exposed to annual concentration of total $PM_{2.5}$ (blue solid line) and dust $PM_{2.5}$ (orange solid line). For comparison, similar CDFs for exposure to total $PM_{2.5}$ (blue dotted line) and dust $PM_{2.5}$ (orange dotted line) defined based on geometric diameter are also shown.

Figure 6: Estimated 2019 cause-specific (a: ALRI, b: CEV, COPD, IHD, and LC and all-cause (f) mortality $\Delta Mort$ attributable to the long-term exposure to total PM2.5. Global total mortality is given in titles of individual panels.

Figure 7: Relative contributions (%) of top 10 countries (colored) and remaining other countries (gray) to global mortality for five specific causes (i.e., ALRI, CEV, COPD, IHD, LC) and all the causes. The number in the center of each pie-chart denotes the total number of global deaths.

Figure 8: 2019 annual average pollution $PM_{2.5}$ (a) and dust $PM_{2.5}$ (b) from MERRA-2 reanalysis.

Figure 9: Estimated 2019 all-cause mortality attributable to (a) pollution $PM_{2.5}$ and (b) dust $PM_{2.5}$. For distributions of cause-specific mortality, please refer to Figures S3 and S4.

Figure 10: Estimated health benefits or global premature deaths (thousands) avoided due to the complete success of enforcing air pollution control worldwide to meet WHO Interim Targets (IT-1, IT-2, IT-3, IT-4) and AQG for annual average $PM_{2.5}$ of 35, 25, 15, 10, and 5 μg m^{-3}, respectively.

Figure S1: Relative risk (RR) as a function of $PM_{2.5}$ concentration (μg m^{-3}) for individual causes of mortality (a) ALRI (b) CEV, (c) COPD, (d) IHD, and (e) LC. The thick line represents the average and shaded area for the upper and lower bounds (to be used for estimating CI95 range of the mortality in this study).

Figure S2: The 2019 baseline mortality counts for individual causes (a – ALRI, b – CEV, c – COPD, d – IHD, and e – LC) and all-cause total (f).

916 **Figure S3:** Cause-specific (a: ALRI, b: CEV, c: COPD, d: IHD, and e: LC) and all-cause (f)
917 mortality attributable to pollution $PM_{2.5}$ in 2019.

918 **Figure S4:** Cause-specific (a: ALRI, b: CEV, c: COPD, d: IHD, and e: LC) and all-cause (f)
919 mortality attributable to dust $PM_{2.5}$ in 2019.

920

921

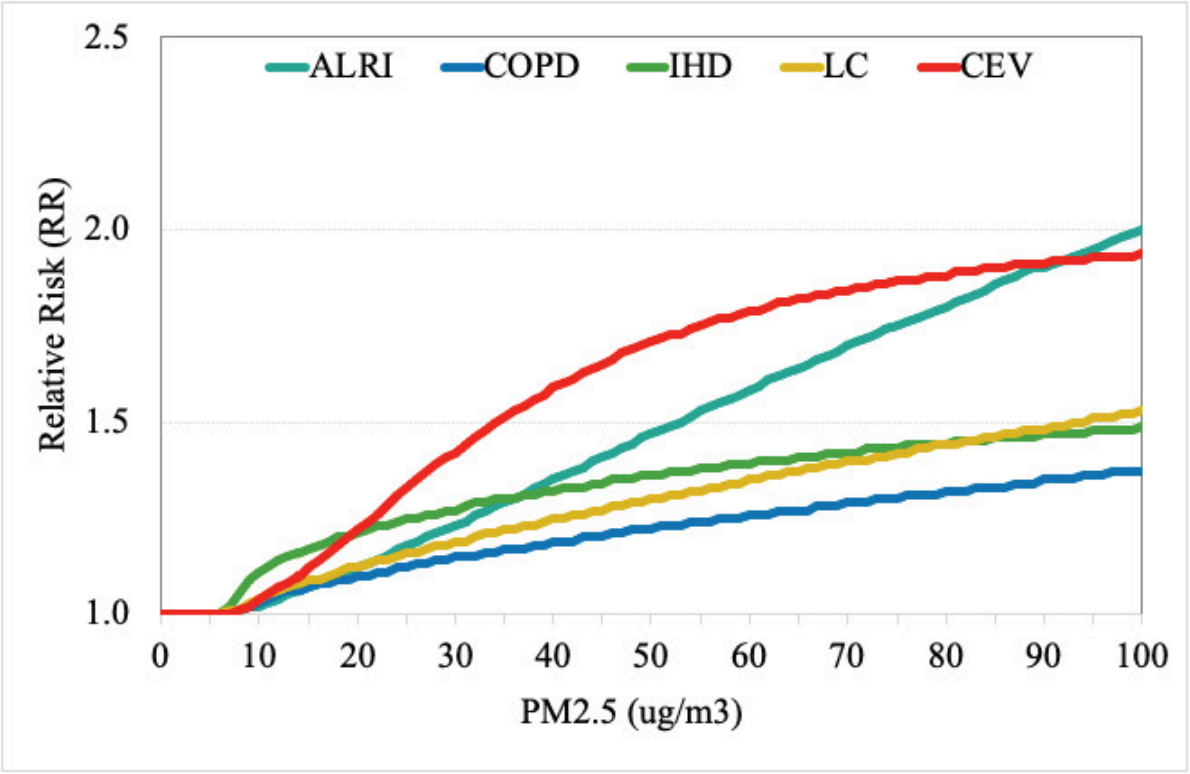

922

923 **Figure 1:** Relative risk (RR) as a function of $PM_{2.5}$ concentration ($\mu g\ m^{-3}$) or concentration-response
924 function (CRF) for individual causes of mortality, including ALRI, COPD, IHD, LC, and CEV.

925

926

927

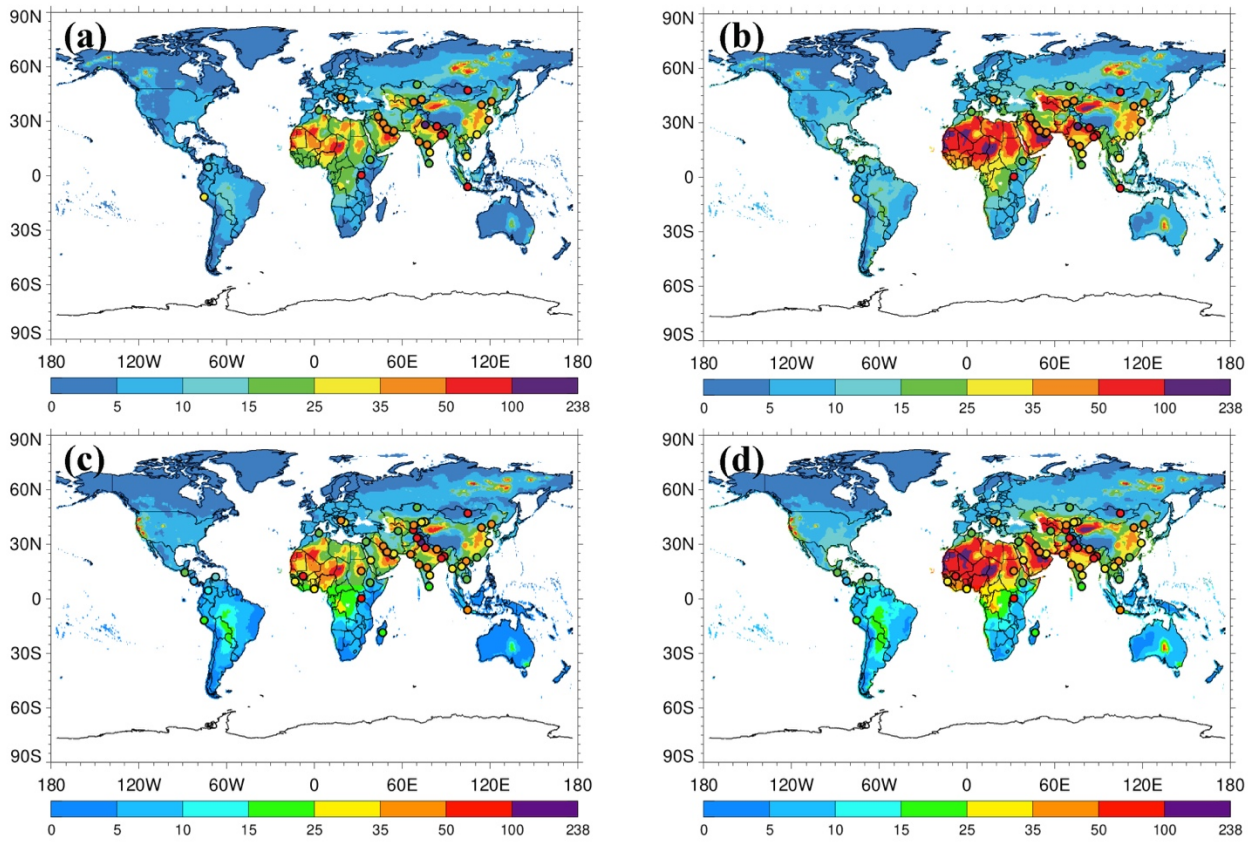

928

929 **Figure 2:** Annual average $PM_{2.5}$ (left panels) and $PM_{2.5}^{geo}$ (right panels) concentrations (μg m^{-3}) from
930 MERRA-2 reanalysis in 2019 (a and b) and 2020 (c and d). $PM_{2.5}$ concentrations measured in the
931 U.S. Diplomatic Posts (greater than 270 days in a year) are overlaid on the MERRA-2 $PM_{2.5}$ maps
932 with the same color scale.

933

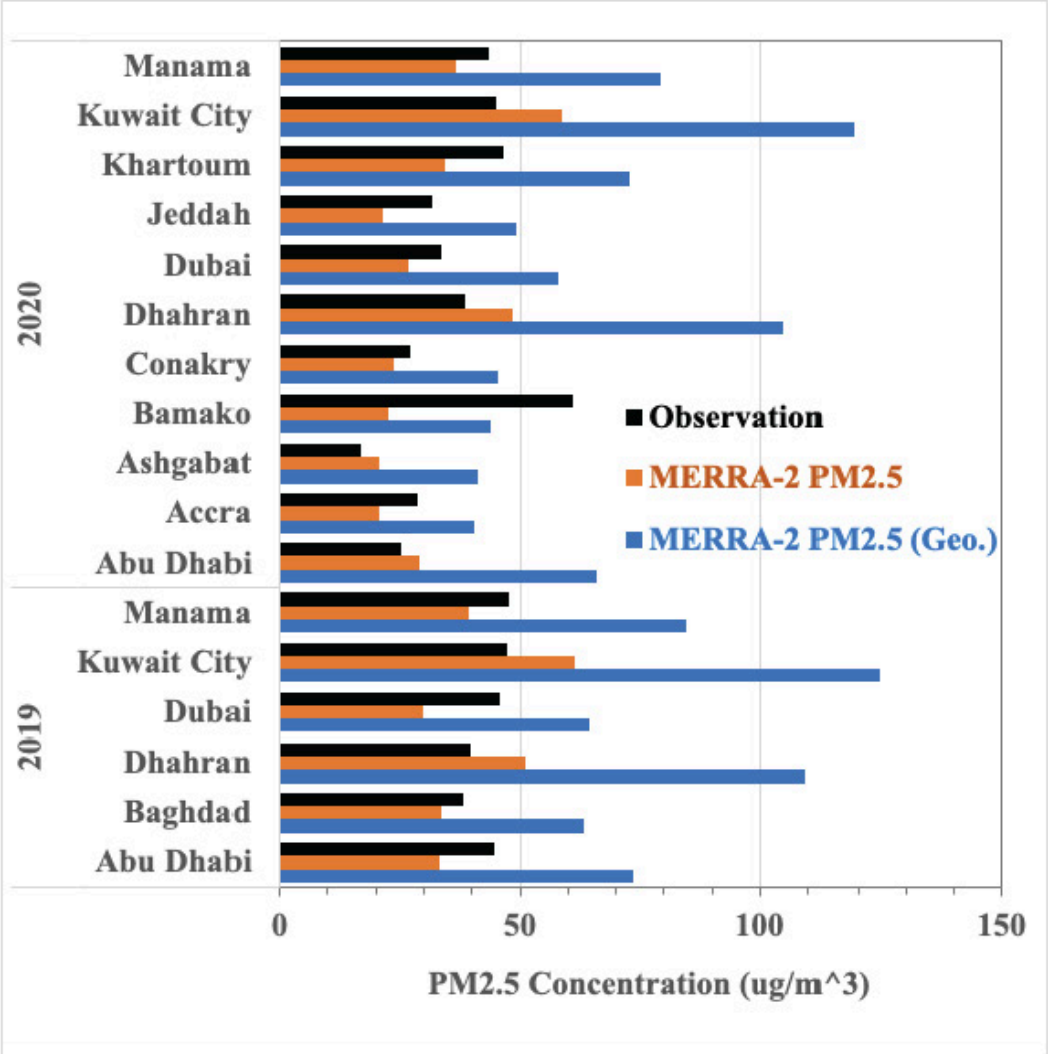

Figure 3: Comparisons of observed $PM_{2.5}$ (black) and MERRA-2 $PM_{2.5}$ (orange) and $PM_{2.5}^{geo}$ (blue) in the heavily dusty U.S. Diplomatic Posts as defined in the text. $PM_{2.5}$ has a unit of μg m^{-3}.

939

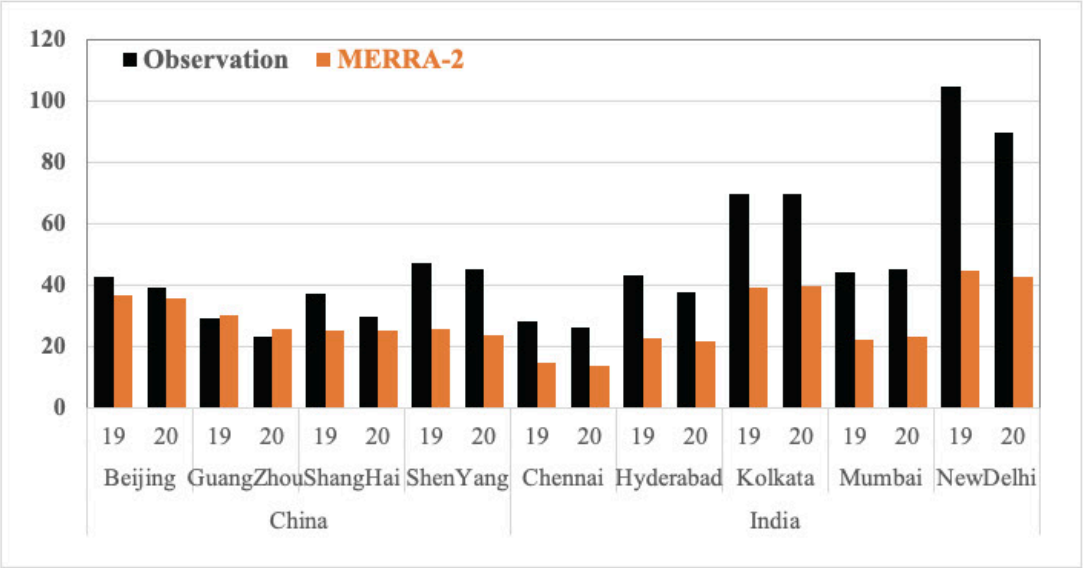

940

941 **Figure 4:** Comparisons of MERRA-2 $PM_{2.5}$ concentration ($\mu g\ m^{-3}$) in 2019 and 2020 with the
942 observations at nine U.S. Diplomatic Posts in China and India.

943

944

945

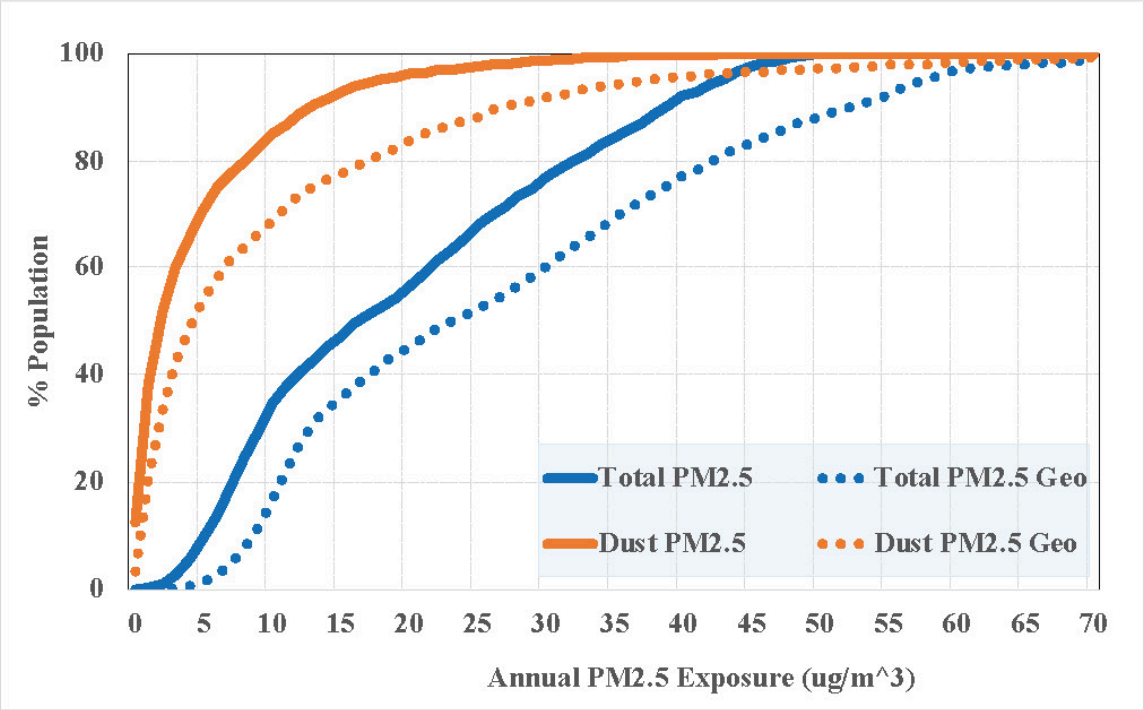

946

947 **Figure 5**: Cumulative distribution functions (CDFs) of population exposed to annual concentration of
948 total $PM_{2.5}$ (blue solid line) and dust $PM_{2.5}$ (orange solid line). For comparison, similar CDFs for
949 exposure to total $PM_{2.5}$ (blue dotted line) and dust $PM_{2.5}$ (orange dotted line) defined based on
950 geometric diameter are also shown.

951

952

953

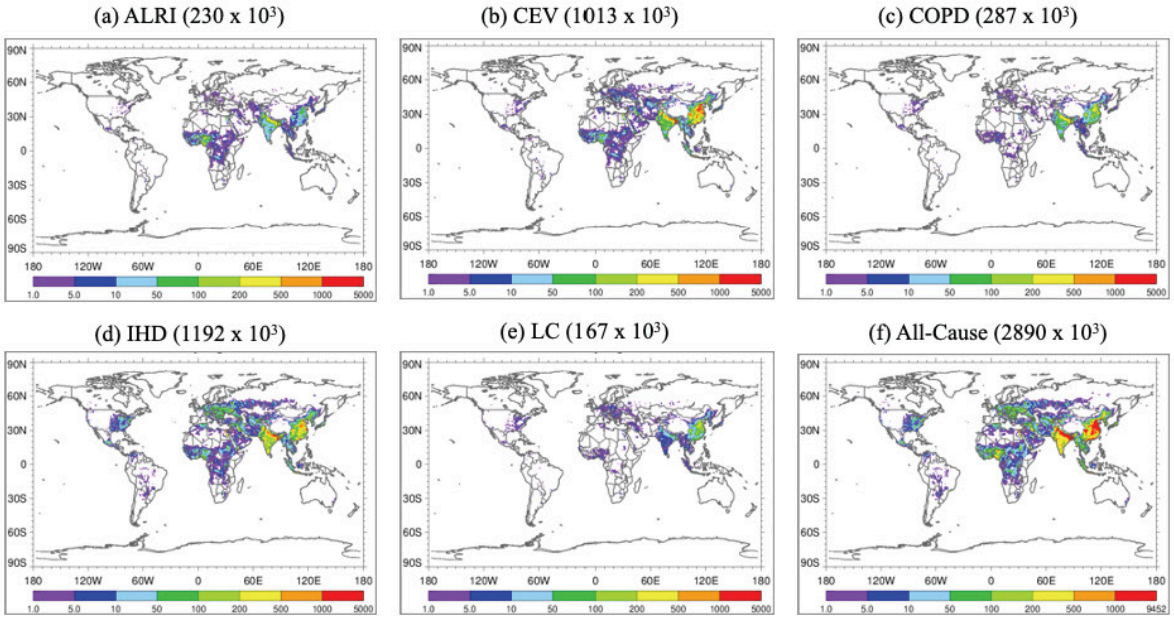

954

955 **Figure 6**: Estimated 2019 cause-specific (a: ALRI, b: CEV, COPD, IHD, and LC and all-cause (f)
956 mortality $\Delta Mort$ attributable to the long-term exposure to total PM2.5. Global total mortality is given
957 in titles of individual panels.

958

959

960

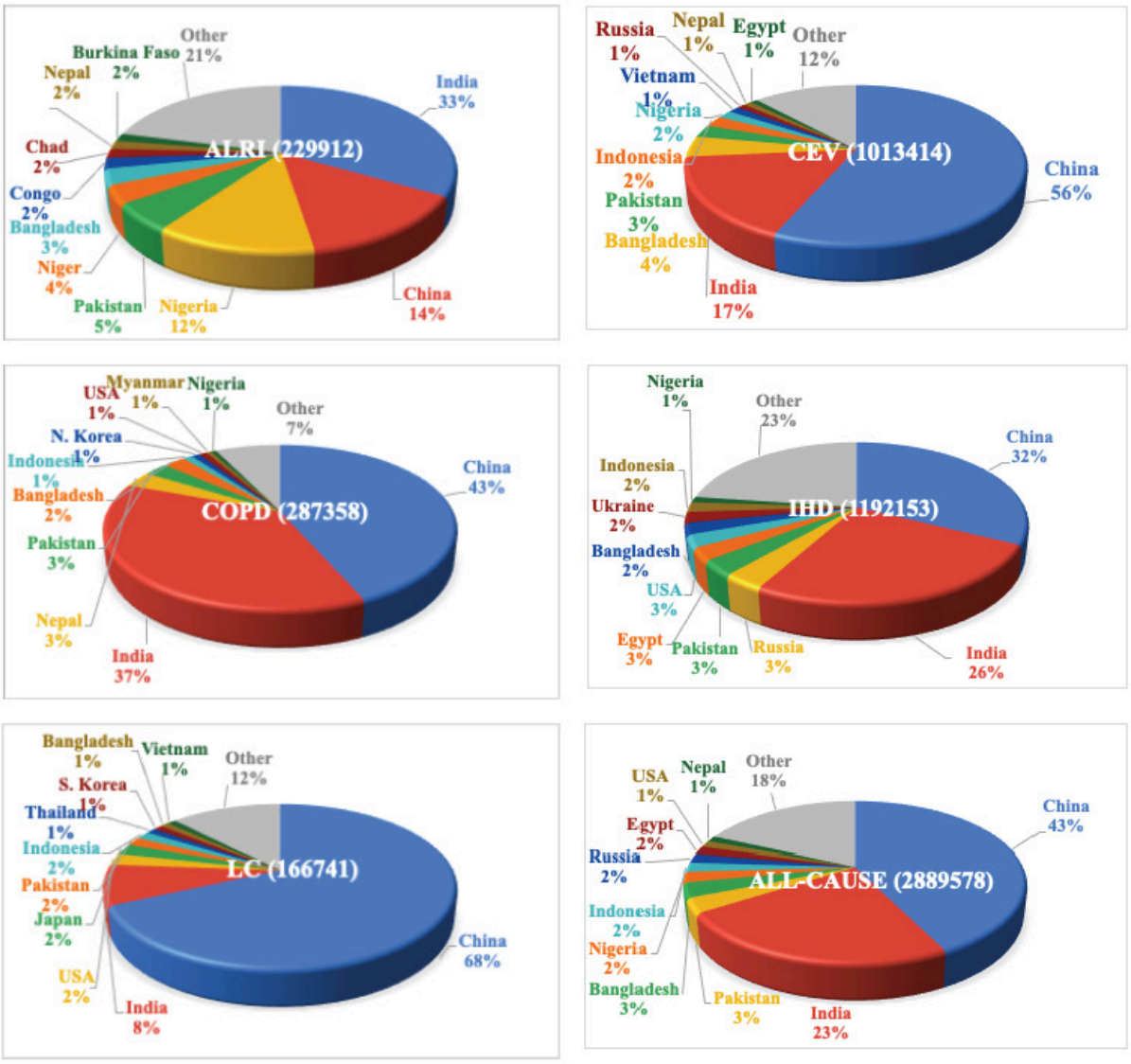

961

962 **Figure 7:** Relative contributions (%) of top 10 countries (colored) and remaining other countries
963 (gray) to global mortality for five specific causes (i.e., ALRI, CEV, COPD, IHD, LC) and all the
964 causes. The number in the center of each pie-chart denotes the total number of global deaths.

965

966

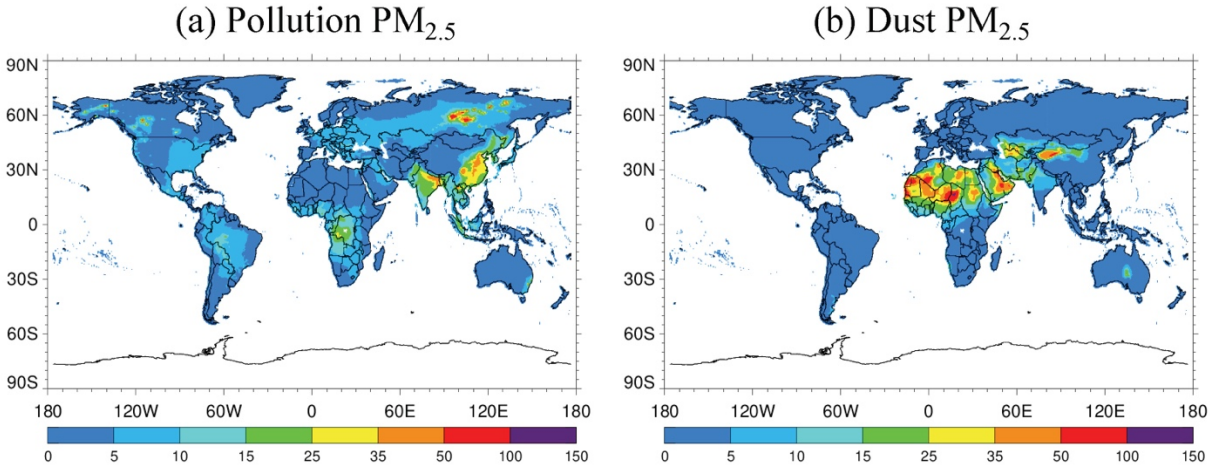

967

968 **Figure 8:** 2019 annual average pollution $PM_{2.5}$ (a) and dust $PM_{2.5}$ (b) from MERRA-2 reanalysis.

969

970

971

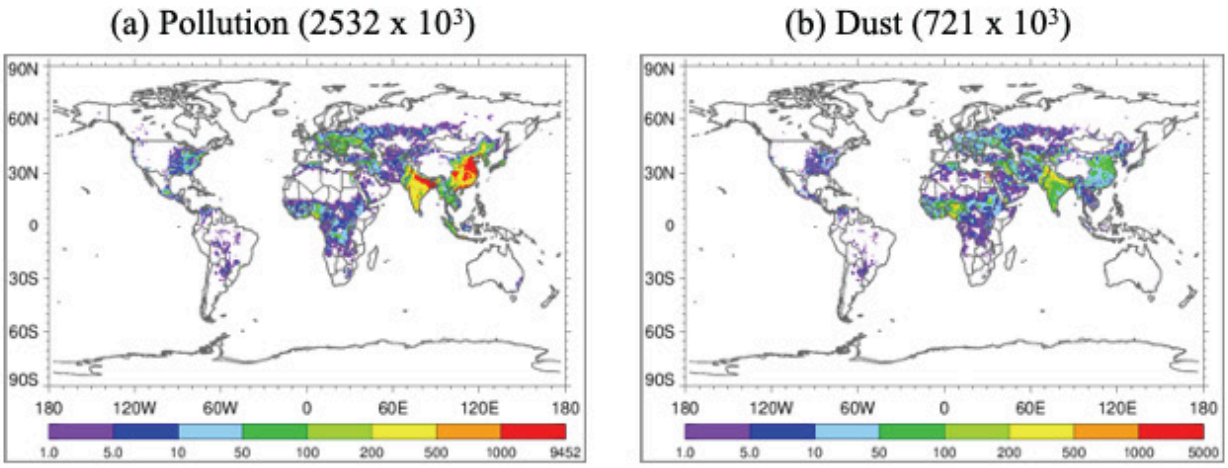

972

973 **Figure 9:** Estimated 2019 all-cause mortality attributable to (a) pollution $PM_{2.5}$ and (b) dust $PM_{2.5}$.
974 For distributions of cause-specific mortality, please refer to Figures S3 and S4.

975

976

977

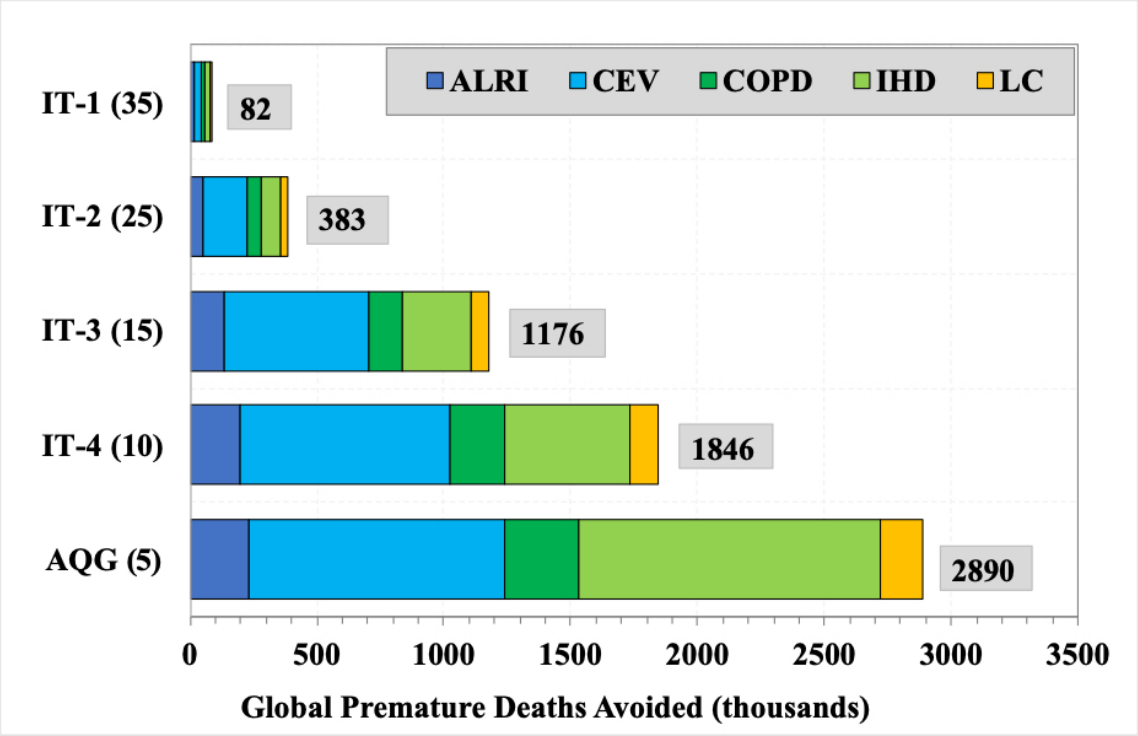

978

979 **Figure 10:** Estimated health benefits or global premature deaths (thousands) avoided due to the
980 complete success of enforcing air pollution control worldwide to meet WHO Interim Targets (IT-1,
981 IT-2, IT-3, IT-4) and AQG for annual average $PM_{2.5}$ of 35, 25, 15, 10, and 5 μg m^{-3}, respectively.

982

983

984

Supplementary Material

Table S1: Annual average $PM_{2.5}$ concentration ($\mu g\ m^{-3}$) measured at the US Diplomatic Posts in 2019 and 2020.

Site name	Lat	Lon	2019	2020
AbuDhabi	24.5	54.4	44.6	25.4
Accre	5.6	-0.2	-	28.6
AddisAbaba	9.0	38.8	20.3	24.3
Algiers	36.8	3.1	21.8	20.3
Almaty	43.2	76.9	-	29
Amman	32.0	35.9	-	20.7
Antananarivo	-18.9	47.5	-	18.6
Ashgabat	38.0	58.3	-	16.8
Baghdad	33.3	44.3	38.3	-
Bamako	12.6	-8.0	-	61.2
Beijing	39.9	116.4	42.7	39
Bishkek	42.9	74.6	35.4	31.6
Bogota	4.7	-74.1	13.0	12.8
Chennai	13.1	80.3	27.9	25.8
Colombo	6.9	79.9	23.5	19.5
Conakry	9.6	-13.6	-	27
Curacao	12.2	-69.0	-	10.4
Dhahran	26.2	50.0	39.7	38.4
Dhaka	23.8	90.4	86.3	84.4
Dubai	25.2	55.3	45.7	33.8
Dushanbe	38.6	68.8	-	53.5
Kathmandu	27.7	85.3	45.7	36.6
Guangzhou	23.1	113.3	29.2	22.8
GuatemalaCity	14.6	-90.5	-	19.3

Hanoi	21.0	105.8	-	43.7
HoChiMinhCity	10.8	106.2	25.9	23.1
Hyderabad	17.4	78.5	43.0	37.6
Islamabad	33.7	73.0	-	46.1
JakartaCentral	-6.2	106.8	40.1	34
JakartaSouth	-6.2	106.8	52.6	41.5
Jeddah	21.5	39.2	-	31.6
Kampala	0.3	32.6	60.5	57.7
Karachi	24.9	67.0	-	48.9
Kathmandu	27.7	85.3	54.5	43.1
Khartoum	15.5	32.6	-	46.6
Kolkata	22.6	88.4	69.3	69.7
KuwaitCity	29.4	48.0	47.2	44.9
Lahore	31.5	74.4	-	104.2
Lima	-12.0	-77.0	30.5	23.4
Manama	26.2	50.6	47.6	43.4
Mumbai	19.1	72.9	43.9	45
NewDelhi	28.6	77.2	104.6	89.3
Nur-Sultan	51.2	71.5	24.1	19.4
Peshawar	34.0	71.5	-	72.2
Pristina	42.7	21.2	25.9	28.4
Rangoon	16.8	96.2	-	28.5
SanJose	9.9	-84.1	-	9.3
Sarajevo	43.9	18.4	37.0	43.8
Shanghai	31.2	121.5	37.1	29.6
Shenyang	41.8	123.4	47.2	45.2
Tashkent	41.3	69.2	41.9	38.1
Ulaanbaatar	47.9	106.9	61.2	52
Vientiane	18.0	102.6	-	32.4

985

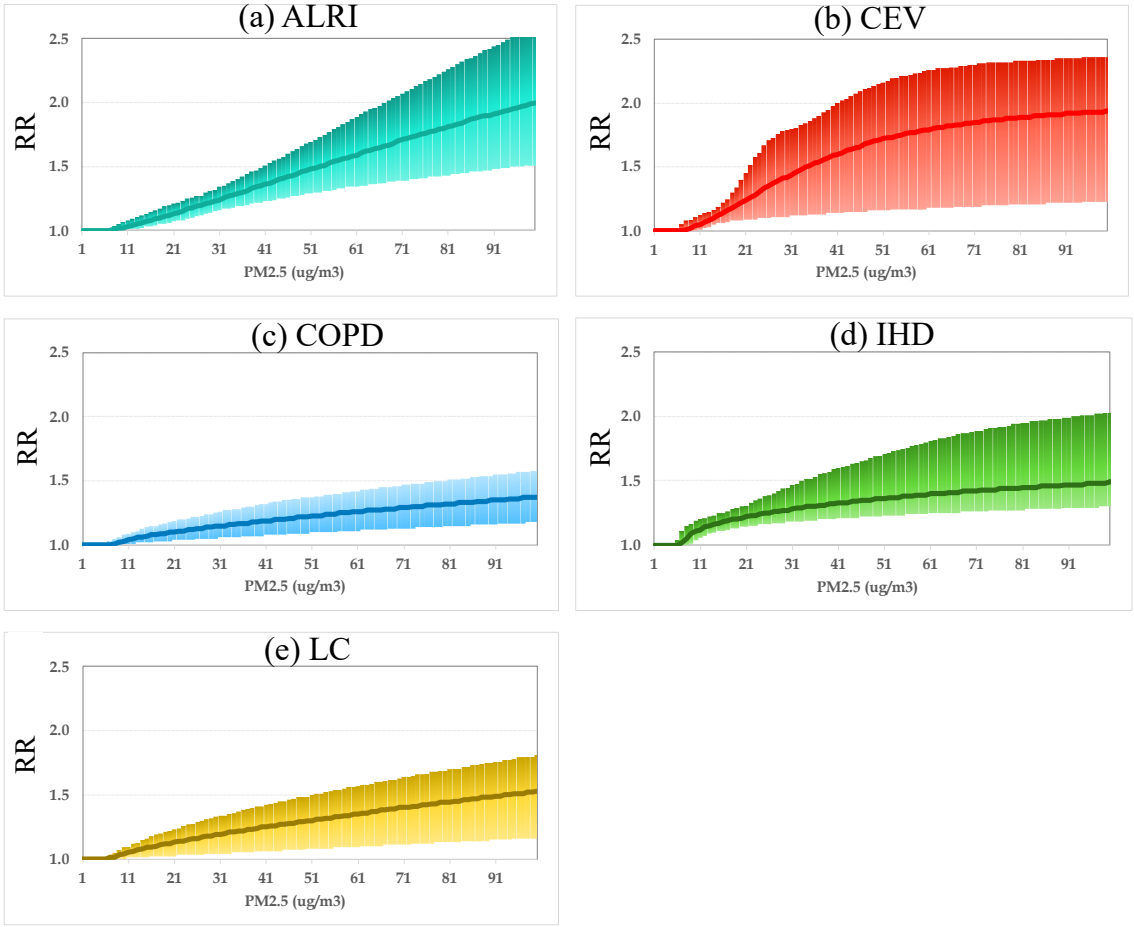

Figure S1: Relative risk (RR) as a function of $PM_{2.5}$ concentration ($\mu g\ m^{-3}$) for individual causes of mortality (a) ALRI (b) CEV, (c) COPD, (d) IHD, and (e) LC. The thick line represents the average and shaded area for the upper and lower bounds (to be used for estimating CI95 range of the mortality in this study).

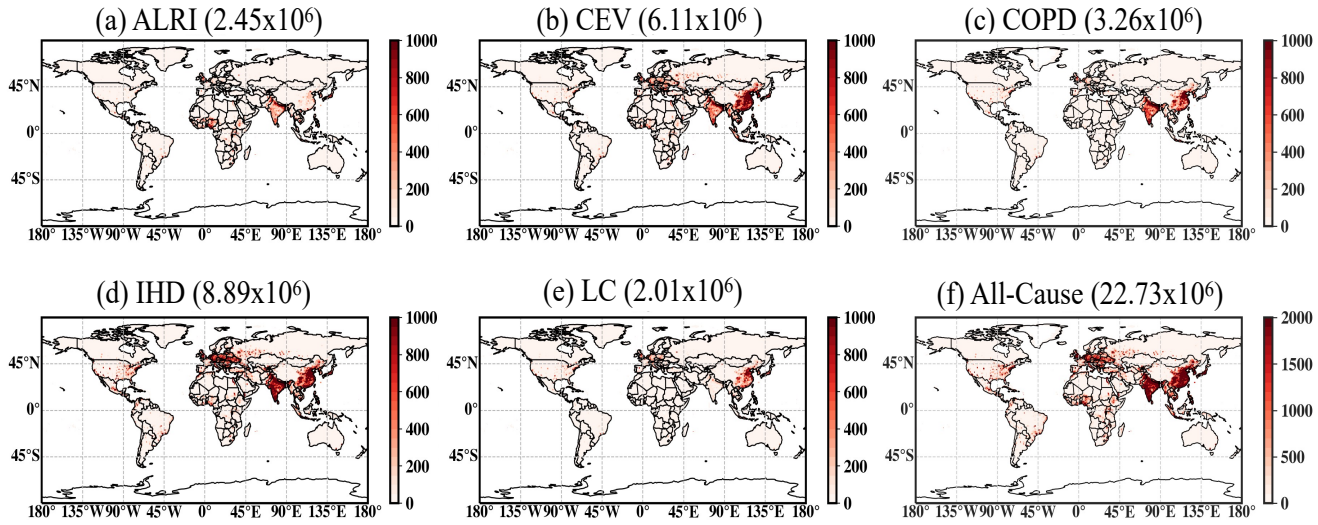

Figure S2: The 2019 baseline mortality counts for individual causes (a – ALRI, b – CEV, c – COPD, d – IHD, and e – LC) and all-cause total (f).

997

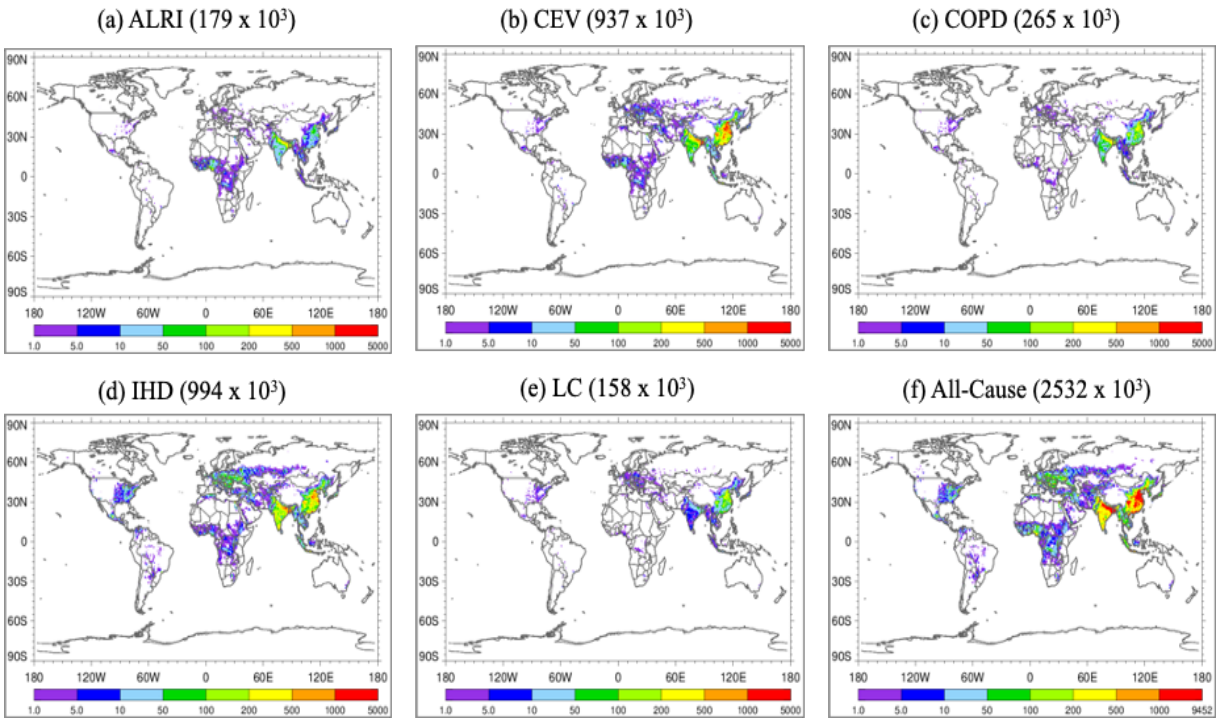

Figure S3: Cause-specific (a: ALRI, b: CEV, c: COPD, d: IHD, and e: LC) and all-cause (f) mortality attributable to pollution $PM_{2.5}$ in 2019.

998

999

1000

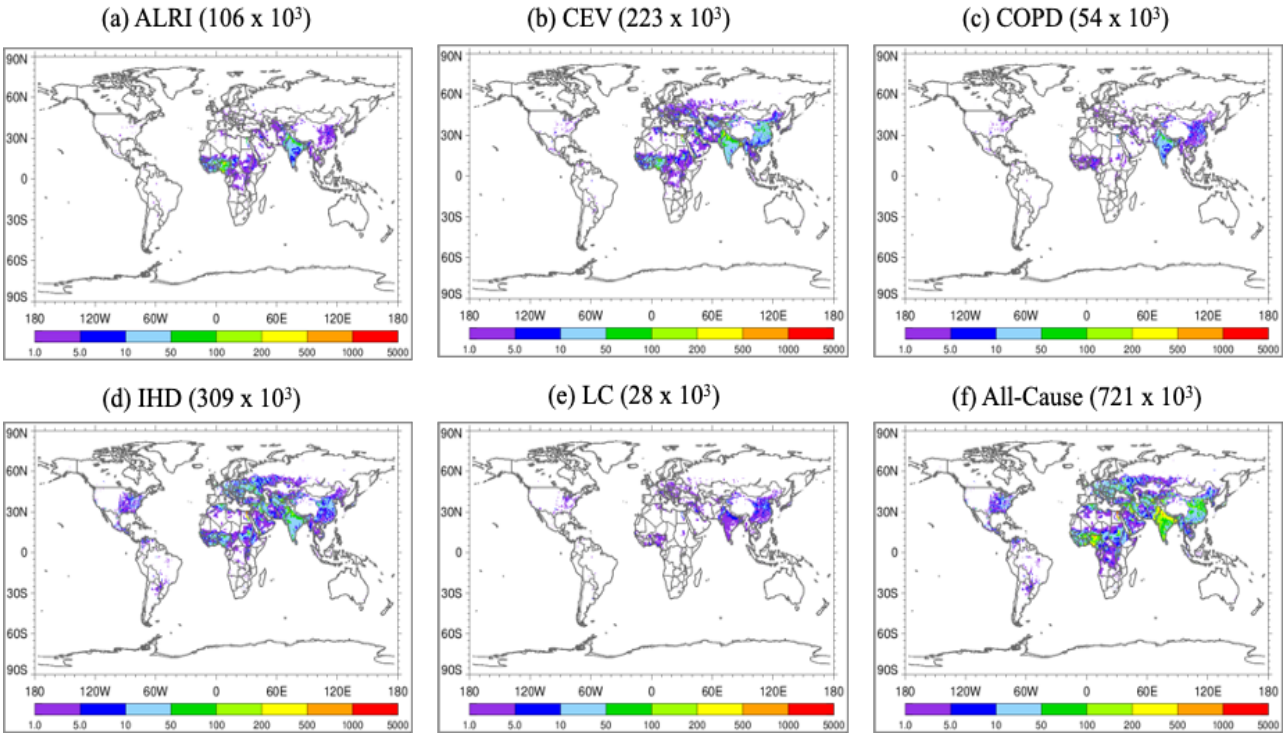

Figure S4: Cause-specific (a: ALRI, b: CEV, c: COPD, d: IHD, and e: LC) and all-cause (f) mortality attributable to dust $PM_{2.5}$ in 2019.

1001